PHASE 2 INITIAL BOREHOLE DRILLING AND TESTING, SOUTH BRUCE

WP04C Data Report: Porewater Extraction and Analyses, and Petrographic Analysis for SB_BH01

APM-REP-01332-0319 December 2023

Geofirma Engineering

NUCLEAR WASTE MANAGEMENT ORGANIZATION
SOCIÉTÉ DE GESTION DES DÉCHETS NUCLÉAIRES

Nuclear Waste Management Organization
22 St. Clair Avenue East, 4th Floor
Toronto, Ontario
M4T 2S3
Canada

Tel: 416-934-9814
Web: www.nwmo.ca

Phase 2 Initial Borehole Drilling and Testing, South Bruce

WP04C Data Report: Porewater Extraction and Analyses, and Petrographic Analysis for SB_BH01

Revision: 0 (FINAL)

NWMO Document: APM-REP-01332-0319

Prepared for:

Nuclear Waste Management Organization
22 St. Clair Avenue East. 4th Floor
Toronto, ON, M4T 2S3

Prepared by:

GEOFIRMA ENGINEERING
1 Raymond St. Suite 200, Ottawa, Ontario K1R 1A2
613.232.2525 613.232.7149 geofirma.com

Project Number: 20-211-1

Document ID: SB_BH01_WP04C_Data_Report_R0

December 18, 2023

Title:	WP04C Data Report: Porewater Extraction and Analyses, and Petrographic Analysis for SB_BH01, Phase 2 Initial Borehole Drilling and Testing, South Bruce	
Client:	Nuclear Waste Management Organization	
Project Number:	20-211-1	
Document ID:	SB_BH01_WP04C_Data_Report_R0	
Revision Number:	0 (FINAL)	Date: December 18, 2023
NWMO Document	APM-REP-01332-0319	
Prepared by:	Chris Morgan, M.A.Sc., P.Geo.	
Reviewed by:	Amy Cartier, B.Sc., G.I.T. and Ian Clark, Ph.D.	
Approved by:	Sean Sterling Sean Sterling, M.Sc, P.Eng., P.Geo. – Project Manager - Principal	

Revision Tracking Table

Revision	Revision Release Date	Description of Modifications/Edits
R0A	August 23, 2023	Initial draft release to NWMO for review
R0B	October 23, 2023	Second draft release to NWMO with initial NWMO comments dispositioned
R0	December 18, 2023	Final Release

TABLE OF CONTENTS

LIST OF FIGURES

APPENDICES

1 INTRODUCTION

Geofirma Engineering Ltd. (Geofirma) completed a drilling and testing program at borehole SB_BH01, northwest of Teeswater, Ontario (Figure 1). This report provides a detailed summary of one component of the Geofirma geoscientific investigation as part of the NWMO Phase 2 Initial Borehole Drilling and Testing Program within the South Bruce site. Specifically, this report describes the activities associated with Geofirma's Work Package 4C (WP04C), which included porewater extraction and analyses, and petrographic analyses for core obtained from borehole SB_BH01.

1.1 Background

Geofirma was retained by the Nuclear Waste Management Organization (NWMO) to complete a drilling and testing program for two deep bedrock boreholes (SB_BH01 and SB_BH02) as part of the NWMO's Phase 2 Geoscientific Preliminary Field Investigations. The full scope of the drilling and testing program for SB_BH01 is described in the Initial Borehole Characterization Plan.

NWMO's process is called the Adaptive Phased Management (APM) plan and comprises multiple phases.

Phase 1 of NWMO's APM plan included preliminary desktop studies using available geoscientific information and a set of key geoscientific characteristics and factors that can be realistically assessed at the desktop phase of the Preliminary Assessment. The Phase 1 Preliminary Assessment of the South Bruce site identified the Cobourg Formation as the preferred host formation for a deep geological repository for used nuclear fuel. The Initial Borehole Drilling and Testing study is a key component of the Phase 2 Geoscientific Preliminary Field Investigations for the NWMO's APM plan.

Borehole SB_BH01 was the first borehole drilled in the South Bruce site as part of the Phase 2 Initial Borehole Drilling and Testing program. SB_BH01 is located approximately 3.5 km northwest of the community of Teeswater, Ontario, and was drilled to 880.84 m below ground surface (m BGS). SB_BH01 was drilled through the entire sedimentary bedrock sequence to approximately 20 m into the Precambrian basement.

1.2 Geologic Setting

The sequence of rocks encountered in the SB_BH01 borehole consist of Paleozoic-aged strata that were deposited within the Michigan Basin northwest of the Algonquin Arch in Southwestern Ontario. The Michigan Basin is a circular-shaped cratonic basin that is composed primarily of shallow marine carbonates, evaporites, and shales that were deposited while eastern North America was in tropical latitudes during the Paleozoic Era (Armstrong and Carter 2010). West of the Algonquin Arch, strata from the Michigan Basin tend to gradually dip westward into the Michigan Basin. Borehole SB_BH01 was drilled through the entire Paleozoic sequence to approximately 20 m into the Precambrian basement, which is composed of high-grade metamorphic rocks of the Grenville Province.

LEGEND

- SB_BH01 Drill Site
- Municipality of South Bruce
- Municipality of Brockton
- Township of Huron-Kinloss
- Provincially Significant Wetland
- Wetland
- Waterbody
- Watercourse
- Major Road
- Local / Street
- OGSRL Well Locations

INSET MAP

Figure 1
Location of SB_BH01 Drill Site

Scale 1:60,000

0 500 1,000 2,000 3,000 4,000
Meters

N

Projection: NAD 1983 UTM Zone 17N

Source: NWMO, Ontario GeoBase

Service Layer Credits: Sources: Esri, HERE, Garmin, Intermap, increment P Corp., GEBCO, USGS, FAO, NPS, NRCAN, GeoBase, IGN, Kadaster NL, Ordnance Survey, Esri Japan, METI, Esri China (Hong Kong), (c) OpenStreetMap contributors, and the GIS User Community

PROJECT No. 20-211-1

NWMO South Bruce
Drilling and Testing

DESIGN: ADG
CAD/GIS: ADG
CHECK: SNS
REV: 0

GEOFIRMA
ENGINEERING

DATE: 2023-10-30

E:\Data\Project\Bruce\Maps\20-211-1_SouthBruce\20-211-1_Figure1_SB_BH01_TestPlans.mxd

1.3 Technical Objectives

The primary technical objective of the WP04C porewater program was to characterize the fluid chemistry of the sedimentary bedrock at the South Bruce site based on core obtained from boreholes SB_BH01 and SB_BH02. This report has been prepared to provide a detailed summary of the sampling methods, laboratory procedures, and results from the WP04C porewater characterization program that was completed for core obtained from borehole SB_BH01.

Results of the porewater and dissolved gas extraction and analysis work will be used as part of data integration activities (Work Package 10) to assess the age of porewater in the Upper Ordovician shale and limestone formations, as well as obtain evidence of whether the porewater has been in contact with modern surface waters.

2 DESCRIPTION OF ACTIVITIES

2.1 Sample Collection and Preservation

2.1.1 Sample Selection and Collection

Selection and collection of porewater, noble gas, and dissolved gas (CO_2 & CH_4) samples were completed by Geofirma staff during drilling of borehole SB_BH01. Intact sections of core were collected as samples according to NMWO-specified geologic/depth interval targets. Samples were collected such that they were representative of the unit being sampled and did not cross a lithological contact. In addition, samples were generally not taken from the immediate top or bottom of a core run to preserve the ability to re-align adjacent core runs by re-fitting the reference line. All samples were extracted using a hammer and chisel, or at pre-existing mechanical/natural breaks.

As much as possible, the porewater, noble gas, and dissolved gas core samples were preserved within 15 minutes of core retrieval, immediately after core run photography, but prior to core logging. All core samples were weighed and photographed prior to preservation.

Core sample locations and procedures for sample collection are described in detail in the Work Package 3 (WP03) Data Report (Geofirma 2022) and the associated WP04C test plan.

2.1.2 Sample Preservation for Paper Absorption, Vacuum Distillation, and Petrography

Samples for paper absorption, vacuum distillation and petrography were collected as porewater samples and were assigned “PW” sample designation using NWMO’s acQuire data management system (e.g., SB_BH01_PW012). A set of two PW samples was collected at each sample location: a 20-30 cm sample for paper absorption and petrography/mineralogy testing, and a second 15 cm sample for vacuum distillation, vacuum distillation leaching, and crush and leach testing. Each set of PW samples was paired with samples for noble gases and dissolved gases (CO_2, CH_4).

The porewater samples were preserved following the standard procedure outline below:

1. Wrap in plastic film
2. Wrap in Polyethylene (PE) bag;
3. Flush with nitrogen, evacuate and heat seal using vacuum sealer;
4. Wrap in second PE bag;
5. Flush with nitrogen, evacuate and heat seal using vacuum sealer;
6. Wrap in aluminum foil pouch;
7. Flush with nitrogen, evacuate and heat seal using vacuum sealer.
8. Refrigerate sample

2.1.3 In-Field Encapsulation for Noble Gases

Core samples collected for noble gas analysis were assigned a “NG” sample designation in acQuire. Noble gas samples were preserved using purpose-built stainless-steel containers following a specialized procedure that was provided to Geofirma by the Noble Gas Laboratory at the University of

Ottawa. Each noble gas core sample was encapsulated in a stainless steel chamber with a flange fitted to a copper-seated high-vacuum valve. The encapsulation and preservation process for noble gas samples is summarized below:

1. Insert core into stainless steel chamber and assemble the chamber.
2. Interface chamber with flushing/evacuating manifold.
3. Flushing-evacuating follows the **1-2 1-2** method.
    - Fill the chamber with high purity nitrogen until 5 PSI on the gauge, **1 minute**.
    - Evacuate the chamber for **2 minutes**.
    - Fill the chamber with high purity nitrogen until 10 PSI above background/atmospheric pressure, **1 minute**.
    - Evacuate the chamber for **2 minutes**.
4. Close the valve on the stainless steel chamber. Ensure the vacuum pump is isolated and remove the chamber from the line.
5. Place a plug and gasket into the valve at the top of the chamber and tighten.
6. Label and store the chambers as required.

Figure 2 provides a schematic of the system that was used to complete encapsulation and preservation of core samples for noble gases at SB_BH01.

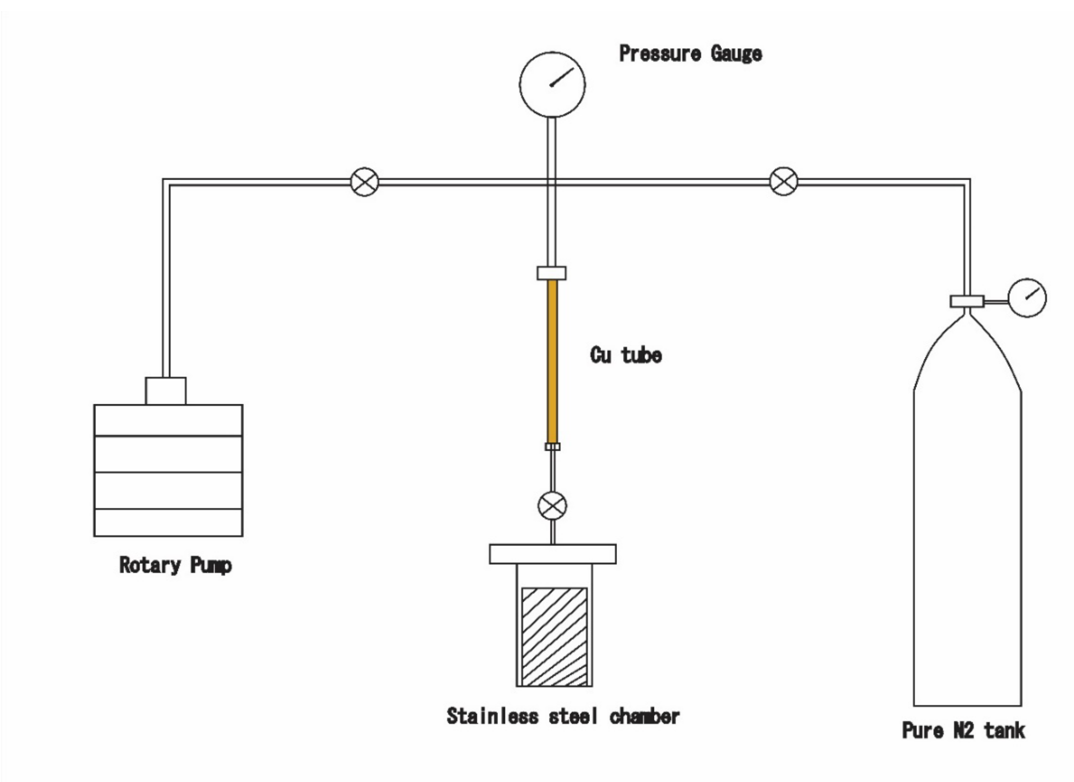

Figure 2 Schematic for noble gas core sample encapsulation (Source: University of Ottawa, Noble Gas Isotope Laboratory)

2.1.4 In-Field Encapsulation for CO_2 and CH_4

Samples for CH_4 and CO_2 analyses were collected as dissolved gas samples and were assigned a “DG” sample designation using acQuire. Full diameter core samples for CH_4 and CO_2 analysis were broken into large chunks (< 5 cm) and placed into two IsoJar (Isotech, USA) containers, capped with a septum-fitted cap. While filling the IsoJar containers, high-purity nitrogen gas was flushed into the containers by a needle through the septum to displace air in the containers. The IsoJars were refrigerated after preservation.

2.2 Sample Processing and Analyses

2.2.1 Vacuum Distillation

Porewater isotopes were sampled from core by vacuum distillation. Vacuum distillation was undertaken on core samples, with the outer perimeter removed and a subsample broken to an approximately sub-centimeter-size fraction. Of this fraction, approximately 30 g per sample was encapsulated in pre-weighed vessels and attached to an extraction line. Evacuation was carried out with a cold trap in place to collect evaporated porewater during evacuation of the line.

The samples were then heated with temperature-controlled ovens to 150°C. This temperature has proven to yield reliable results for the Ordovician shales and carbonates at the Bruce Site (Clark et al., 2013) and for the Tournemire argillite (Altinier et al., 2006). Samples were monitored during a 6-hour distillation period after which the recovered porewater was transferred to 12 mL Exetainers with septum for analysis of $\delta^{18}O$ and $\delta^{2}H$. These isotopes were measured by off-axis integrated cavity output laser spectroscopy using a Los Gatos Research Inc. (LGR) instrument operating in the Ján Veizer Stable Isotope Laboratory at the University of Ottawa. The water vapour distilled from the core material was condensed in a septum vial and weighed for gravimetric water content. The measured water content was compared with the weight loss in the core material to assess water recovery. Samples are run in quadruplicate, using 30 g splits from a single core sample.

2.2.1.1 *Vacuum Distillation Leaching*

The primary method for determination of major/minor ion chemistry of the porewaters was the vacuum distillation leaching (VDL) method. The extraction vessel and dry core material following vacuum distillation were rinsed with distilled water into a pre-weighed falcon tube for out-diffusion of porewater salts. The mass of leach water was recorded and then monitored over time until a stable electrical conductivity was attained. The leach water was then filtered and analyzed for major and trace solutes.

Solute masses, determined from concentration and leach water mass, were normalized to the water mass recovered from distillation to determine total porewater concentrations. Leach water was analyzed (ICP-MS, ICP-OES, IC) for major, minor and trace metals (Na, K, Mg, Ca, Sr, plus Al, Fe, Mn Li, Rb, and Si) as well as major and minor anionic species (B, Cl, Br, I, S) in the Geochemistry Laboratory at the University of Ottawa.

2.2.2 Paper Absorption

A second method, paper absorption (PA), was used to complement and allow comparison with the VDL results for porewater samples. The PA method (Celejewski et al., 2014, 2018) was developed for extraction of mobile porewater for analysis of major anions and cations. The *mobile porewater* is that which is free to flow among the largest pores, and it is a fraction of the *total porewater* which also includes water in clay interlayers and in the electric double layer adjacent to mineral surfaces.

For the PA method, preserved, saturated core sections of minimum 20 cm length were broken in two, and then reassembled with a cellulosic paper placed between the two pieces, and tightly bound. Reassembled cores were left for a period of approximately two months to allow capillary uptake of porewater into the filter paper. When reopened, the recovered filter paper was leached to remove solutes and the leached solution was analyzed (ICP-MS, ICP-OES, IC) to determine the extracted masses of major, and some minor elements (Na, K, Mg, Ca, Li, Sr and Ba) as well as major and minor anionic species (Cl, Br, S) at the University of Ottawa. The mass of absorbed water was determined by near-infrared spectrometry, before and after insertion in the core. The mass of extracted water, after 2 months, represents porewater uptake and was used to convert the solute masses to concentrations.

2.2.3 Analysis for CO_2 and CH_4

Headspace gas in the Isojars was periodically analyzed for concentrations of CH_4 and CO_2 by gas chromatography. When stable concentrations were attained (three successive measurements within analytical uncertainty), the headspace was sampled and analyzed for $\delta^{13}C$ and $\delta^{2}H$ of CH_4 and for $\delta^{13}C$ of CO_2 by routine isotope ratio mass spectrometry at Jan Veizer Stable Isotope Laboratory, University of Ottawa.

2.2.4 Analysis for Noble Gases

All noble gas concentrations were measured on a Thermo-Finnigan Helix SFT noble gas mass spectrometer at the University of Ottawa Lalonde noble gas laboratory using aliquots from the stainless-steel encapsulation chamber. The out-diffused gases were treated with a Ti getter pump maintained at 450°C to remove non-inert gases (principally CH_4 and CO_2). The noble gases were then cryogenically separated by freezing Ar, Kr, and Xe on charcoal traps before sorbing Ne and He on a 5 K cold-head. He and Ne were successively released to the mass spectrometer by ramping the cold-head temperature accordingly. The isotopes of Ar, Kr and Xe were then analyzed.

2.2.5 Analysis for Radiohalides and Strontium Isotopes

Pieces of the core samples were crushed in an aerobic glove box, followed by leaching with an equal mass of deionized and distilled water. These crushed and leached samples were used to extract porewater for radiohalide analyses (^{129}I, ^{36}Cl, and $\delta^{37}Cl$). Sampled water for ^{129}I was treated to precipitate AgI target material and analyzed by the Dresden AMS laboratory in Germany. Sampled water for ^{36}Cl was treated to precipitate AgCl target material which was subsequently analyzed on a high energy AMS system at the Lawrence Livermore National Laboratories facility in California. Water for $\delta^{37}Cl$ analysis and $^{87}Sr/^{86}Sr$ isotope ratios for porewater samples were analyzed at Isotope Tracer Technologies Inc., Waterloo. Part of the leached solution extracted using the PA technique was also used for Sr isotope analyses at the Carleton University Isotope Geochemistry and Geochronology Research Centre.

2.3 Mineralogy and Petrography

Mineralogical and petrological analyses were completed on a subset of porewater samples by the University of Ottawa to obtain mineralogical data required for interpretation and geochemical modelling of the porewater results. Rock core samples that were used for PA analyses were also used for the mineralogical and petrophysical analyses. Thin sections were cut for petrographic analyses and a subsample of core was crushed and milled into a powder for x-ray diffraction (XRD).

Using prepared thin sections, optical mineralogy, scanning electron microscope and energy dispersive x-ray spectrometry (SEM-EDS) were completed. SEM-EDS imaging was completed at the University of Ottawa using a JEOL6610LV SEM operated at an accelerating voltage of 20 Kv and equipped with an EDAX EDS system. The XRD analyses were also completed at the University of Ottawa using a Rigaku Ultima IV diffractometer with a monochromatic CuKα radiation at 40 Kv, 200 Ma.

3 RESULTS

3.1 Porewater Geochemistry

Results from the SB_BH01 porewater characterization program are summarized in the following section, with select mineralogical, geochemical, and isotopic results presented as profiles with depth. A summary of the porewater sample information, including sample type, depth, and logged primary lithology is included as a table in Appendix A. Complete results from the porewater characterization program are provided in Appendix B.

The results presented in this data report have not been corrected for potential mineral dissolution during analyses, apparent halite undersaturation, or anion exclusion. These processes were shown to impact geochemical results for porewater samples that were collected from the similar strata to what was encountered in SB_BH01 as part of the Ontario Power Generation (OPG) Deep Geological Repository site characterization program (Intera 2011). The Intera (2011) report showed that the relative magnitude of impact from these processes, and the corrections that were required to obtain representative porewater concentrations, depended on the porewater chemistry and the sampled lithology/mineralogy.

Detailed interpretation of the porewater results, including geochemical modelling and correction for mineral dissolution, halite under saturation, and anion exclusion will be completed separately as part of Work Package 10 (Data Integration) activities.

3.1.1 Major/Minor Ions and Total Dissolved Solids

Figure 3 presents depth profiles of chloride (Cl), sodium (Na), and calculated total dissolved solids (TDS) measured using both the VDL and PA methods. The TDS values shown in Figure 3 were calculated assuming a fresh-water density and overestimate the true TDS for brackish water to brines that are encountered in many of the samples.

Concentrations of Cl and Na are generally low through the shallow Devonian to the top of the Salina Group. Na and Cl concentrations in the Guelph Formation were low relative to other samples from the overlying/underlying units. Below the Guelph Formation, porewater concentrations of Na and Cl generally increase with depth through the lower Silurian units and the Ordovician-aged shales (Queenston, Georgian Bay, and Blue Mountain formations) to the top of the Cobourg Formation. From the Cobourg Formation to the Shadow Lake Formation, Na and Cl concentrations remain high with some scatter.

Since Na and Cl generally dominate the ionic composition of porewaters, particularly below the Salina Group, the TDS depth profiles show similar trends to the Na and Cl depth profiles. VDL-derived TDS values were below 10 g/L in the Devonian units, between 18-111 g/L in the Salina Group and Guelph Formation, and increased to approximately 250-350 g/L below the Georgian Bay Formation.

Comparison of Cl and Na concentrations measured using the VDL and PA methods show substantial variation, with PA-derived concentrations that were 1-3 orders of magnitude higher than corresponding concentrations obtained using the VDL method. Many of the PA-derived concentrations were supersaturated relative to halite solubility. The significant variation in porewater concentrations that is observed between these two methods may reflect differences in the proportional uptake of clay-bound, capillary-bound, and mobile porewaters.

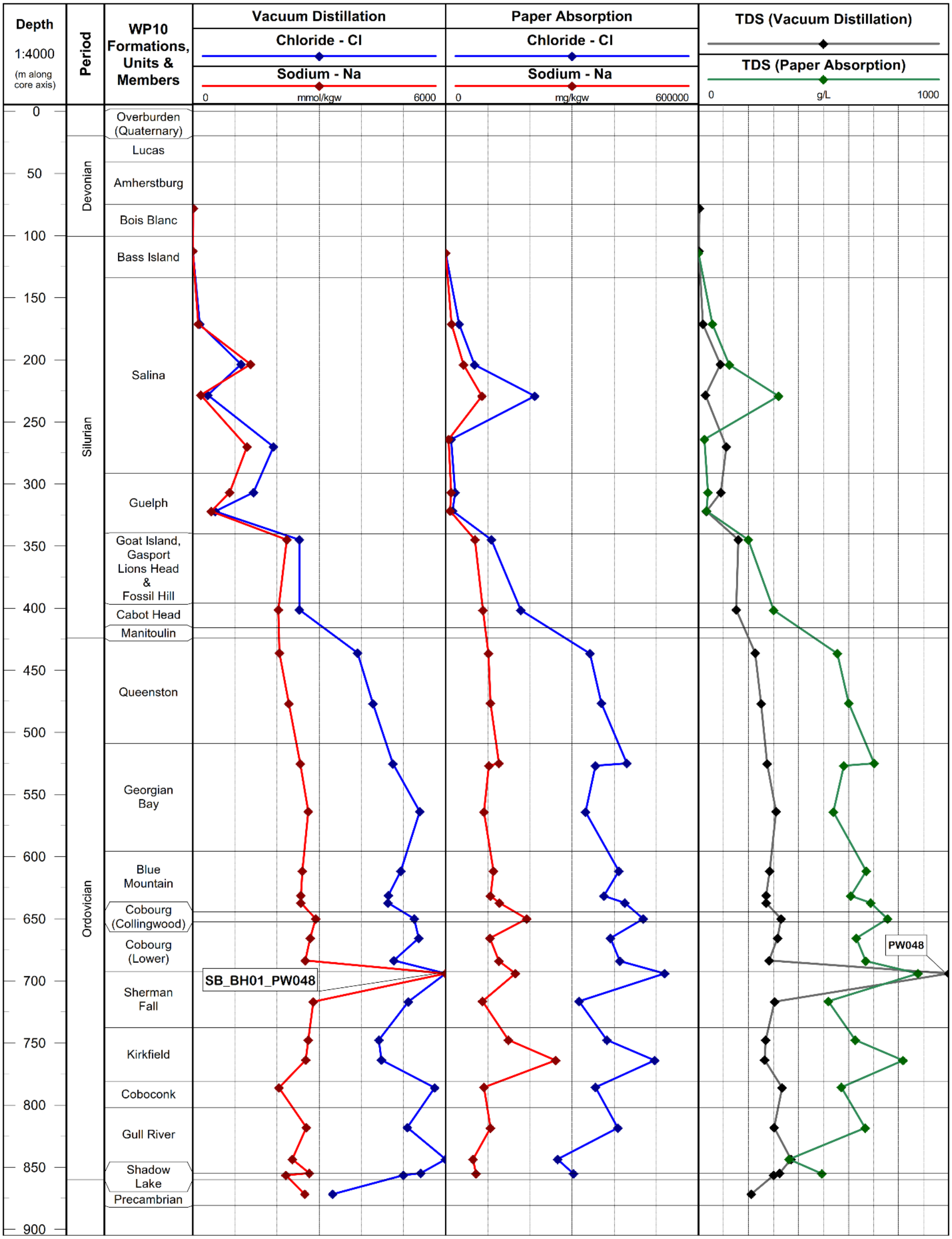

Figure 3 Profile of Chloride, Sodium, and TDS Concentrations of Porewater from Vacuum Distillation and Paper Absorption, SB_BH01 Core Samples. TDS calculated assuming freshwater density (1000 kg/m^3). Sample SB_BH01_PW048 was noted to have exceptionally low water content and strong degassing during sampling.

VDL-measured concentrations of Na, Cl, and other major ions were very high and outside of the anticipated range for a porewater sample that was collected at the top of the Sherman Fall Formation (SB_BH01_PW048). Field observations during core logging and sampling indicated strong degassing of methane from the sample. This sample also has the lowest water content in the section (Appendix B).

Figure 4 shows depth profiles for porewater concentrations of calcium (Ca), magnesium (Mg), and strontium (Sr) measured by VDL. These three elements show similar depth profiles, with low, increasing concentrations through the shallow bedrock to the top of the Salina Group. Samples from the Guelph Formation to the bottom of the Silurian strata show relatively low concentrations of Ca, Mg, and Sr, compared to the overlying and underlying strata. Except for the anomalous sample collected at the top of the Sherman Fall Formation (SB_BH01_PW048), porewater concentrations of Ca, Mg, and Sr, are stable, or increase gradually from the top of the Queenston Formation to the base of the Kirkfield Formation. Concentrations of Ca, Mg, and Sr are higher in the Coboconk and Gull River relative to porewater in the overlying strata, and then decrease rapidly in the basal Shadow Lake Formation and crystalline rocks of the Precambrian basement.

Figure 5 shows depth profiles for porewater concentrations of potassium (K), bromine (Br), and boron (B) measured by VDL. K and Br show similar trends at shallow to intermediate depths, with relatively low concentrations through the Devonian and Silurian-aged strata and increasing concentrations across the Ordovician shales. Concentrations of K remain high, with some scatter, from the Cobourg through to the Sherman Fall Formation, then decline and stay relatively low in the Coboconk, Shadow Lake, and Precambrian. In contrast, porewater Br concentrations remain relatively consistent across all the Ordovician-aged strata, before dropping off in the Precambrian.

Except for one sample from the middle of the Salina Group (SB_BH01_PW008), boron (B) concentrations in porewater are low through the shallow bedrock to the Guelph Formation. From the Goat Island/Gasport Formation through to the base of the Blue Mountain, B concentrations remain relatively low and stable. Boron concentrations in the Ordovician-aged limestones and the Precambrian are higher and show more scatter than in the overlying strata.

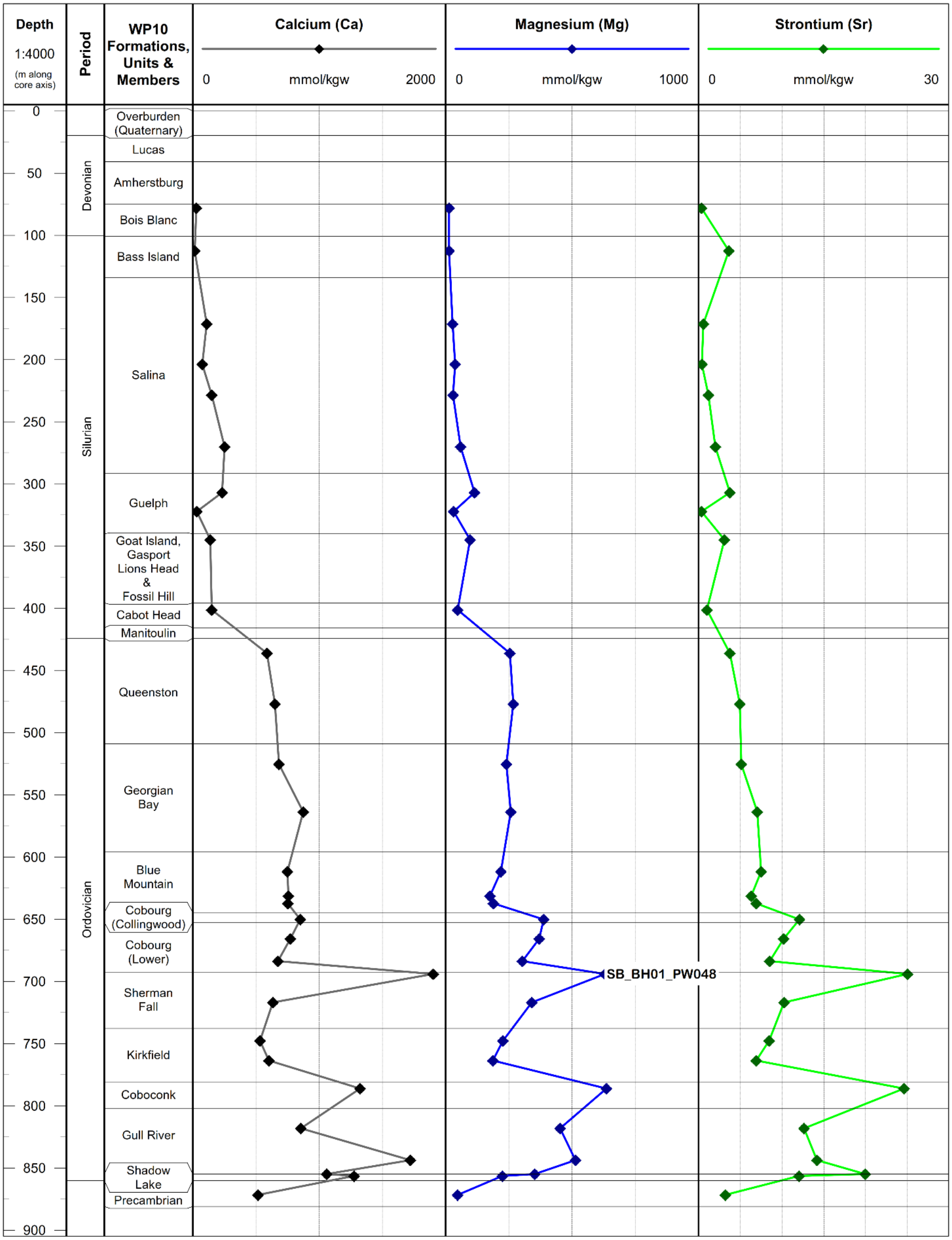

Figure 4 **Profile of Calcium, Magnesium, and Strontium Concentrations in Porewater from Vacuum Distillation, SB_BH01 Core Samples.** Sample SB_BH01_PW048 was noted to have exceptionally low water content and strong degassing of methane during sampling.

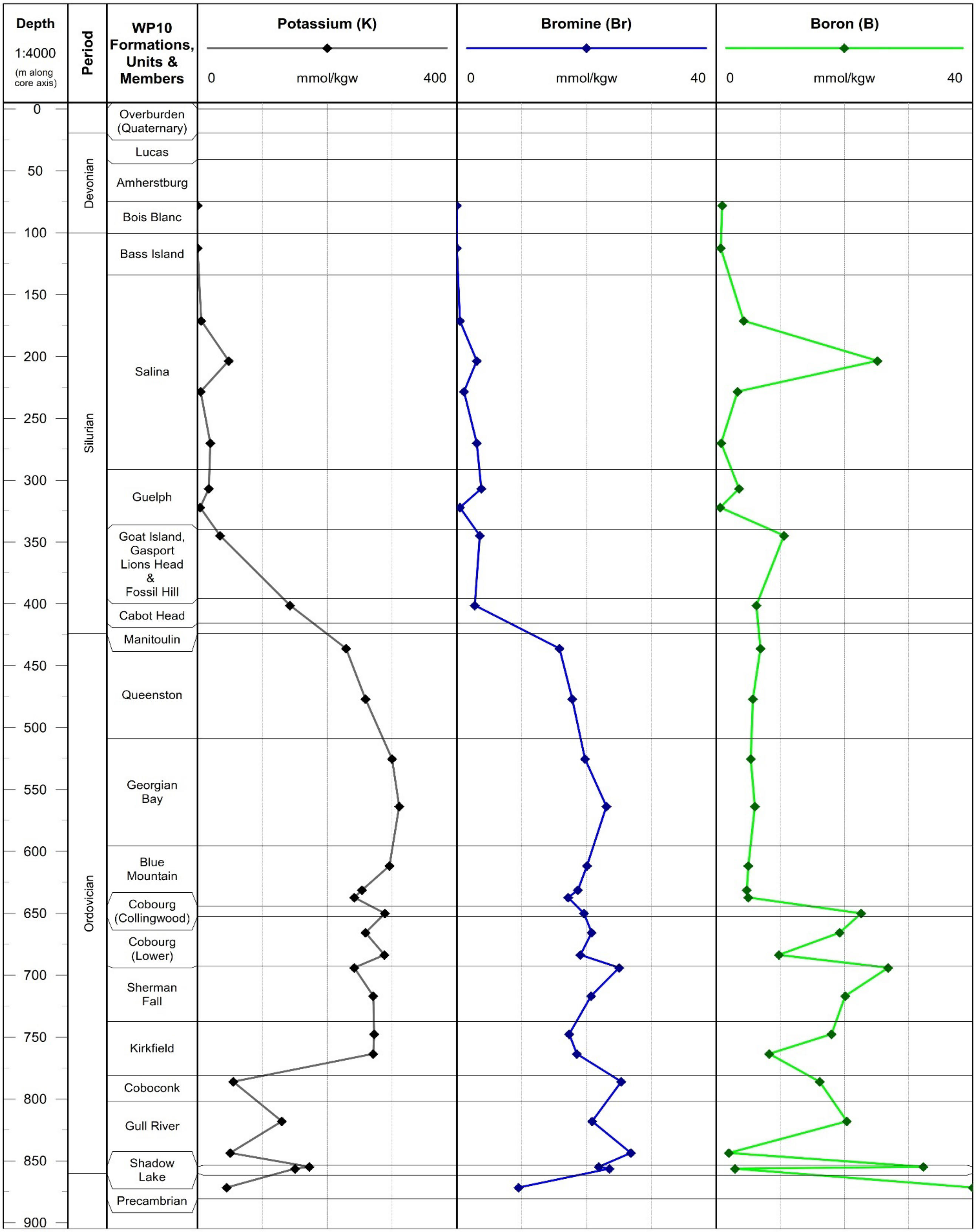

Figure 5 **Profile of Potassium, Bromine, and Boron Strontium Concentrations in Porewater from Vacuum Distillation, SB_BH01 Core Samples**

3.1.2 Environmental Isotopes

Figure 6 shows a cross plot of isotopic ratios for deuterium (^{2}H) and ^{18}O for porewater extracted by vacuum distillation. The accompanying laboratory report for the environmental isotopes had several results that were flagged due to interpreted trace hydrocarbon contamination, but comparison of the results to trends in a depth profile for δ^2H and δ^{18}O (Figure 7) suggests that the magnitude of contamination for the impacted samples is not significant.

Except for SB_BH01_PW008, SB_BH01_PW048 and SB_BH01_PW055, the porewater samples tended to plot adjacent to, or below, the global meteoric water line (GWML). When compared to other samples, sample SB_BH01_PW008 was highly depleted in^{18}O relative to the δ^2H ratio. Such samples observed in the Bruce DGR program (Intera 2011) were attributed to gypsum hydration. Sample SB_BH01_PW048 from the Sherman Fall was the least depleted in ^{18}O of the samples that were collected at SB_BH01 and plots far to the right of the GWML. This sample was noted above for its very high Na and Cl content, which is possibly an artifact of the very low water content in this sample (less than 0.1 percent). The lab reported that this core was likely compromised, the low water content and ^{18}O depletion is consistent with evaporation loss.

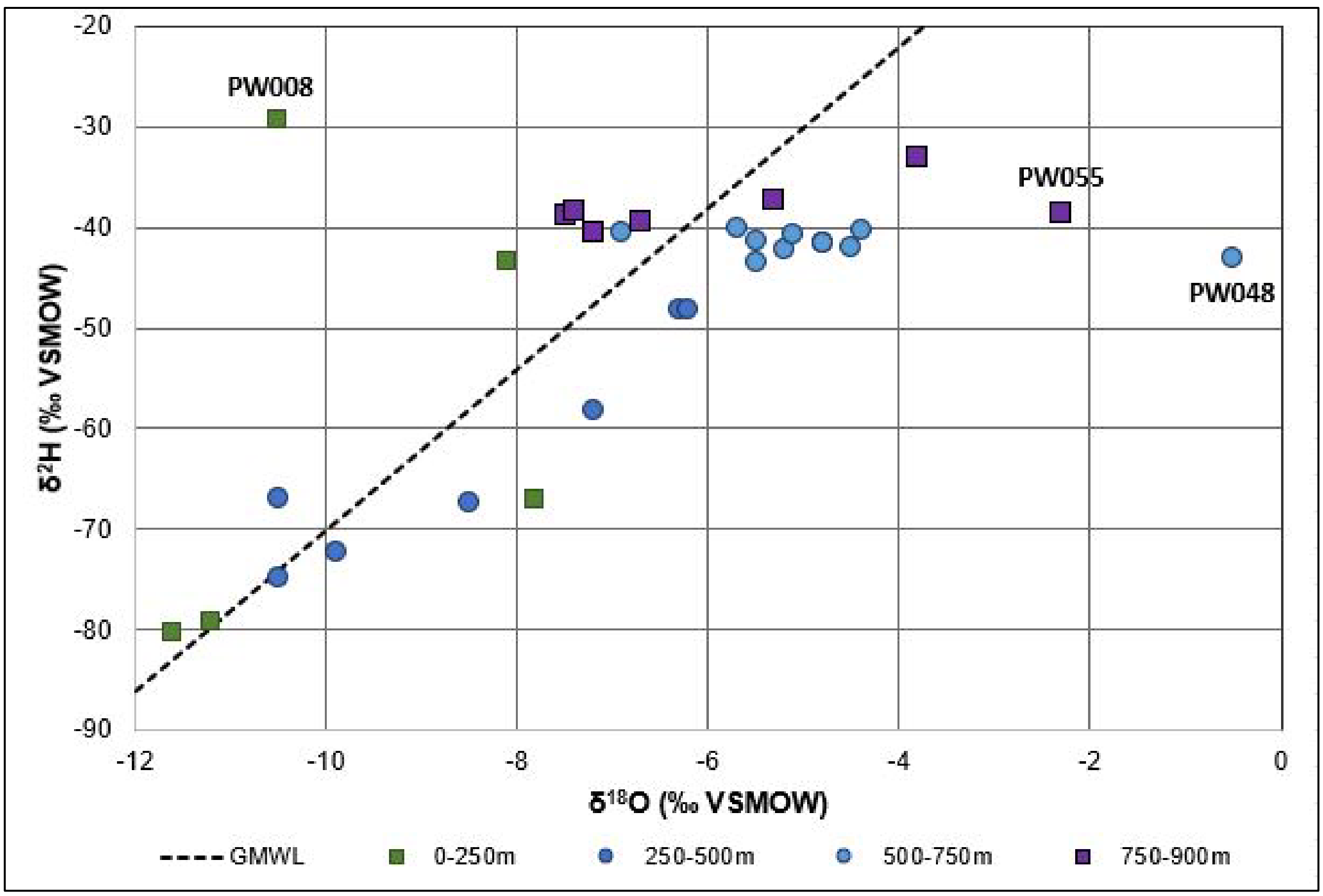

Figure 6 **^{18}O-^{2}H Cross Plot, SB_BH01 Porewater Samples.** Samples SB_BH01_PW048 and SB_BH01_PW055 were noted to have low water content (<0.1% and 0.2%, respectively). Subsamples of SB_BH01 PW055 were combined to have sufficient volume for analysis.

Figure 7 shows depth profiles for $\delta^{18}O$ and $\delta^{2}H$. Samples from the shallow bedrock and the lower Silurian units were the most depleted in both ^{18}O and ^{2}H. Separating these relatively depleted intervals are samples from the top of the Guelph and Salina Group, which were less depleted in both ^{18}O and ^{2}H, including notably ^{2}H in sample SB_BH01_PW008 from the middle of the Salina Group. After a sharp increase in ^{2}H at the top of the Queenston Formation, ^{2}H ratios remain relatively stable and become slightly less depleted with depth. There is also a sharp increase in ^{18}O at the top of the Queenston, followed by steadily increasing concentrations to the Cobourg Formation. Below the Cobourg Formation ^{18}O ratios show significant scatter, with a generally decreasing trend. Sample SB_BH01_PW048 with enriched ^{18}O, discussed above, is observed at the top of the Sherman Fall, along with sample SB_BH01_GW055 with enriched ^{18}O in the upper Coboconk Formation, which also had an effect from very low water content.

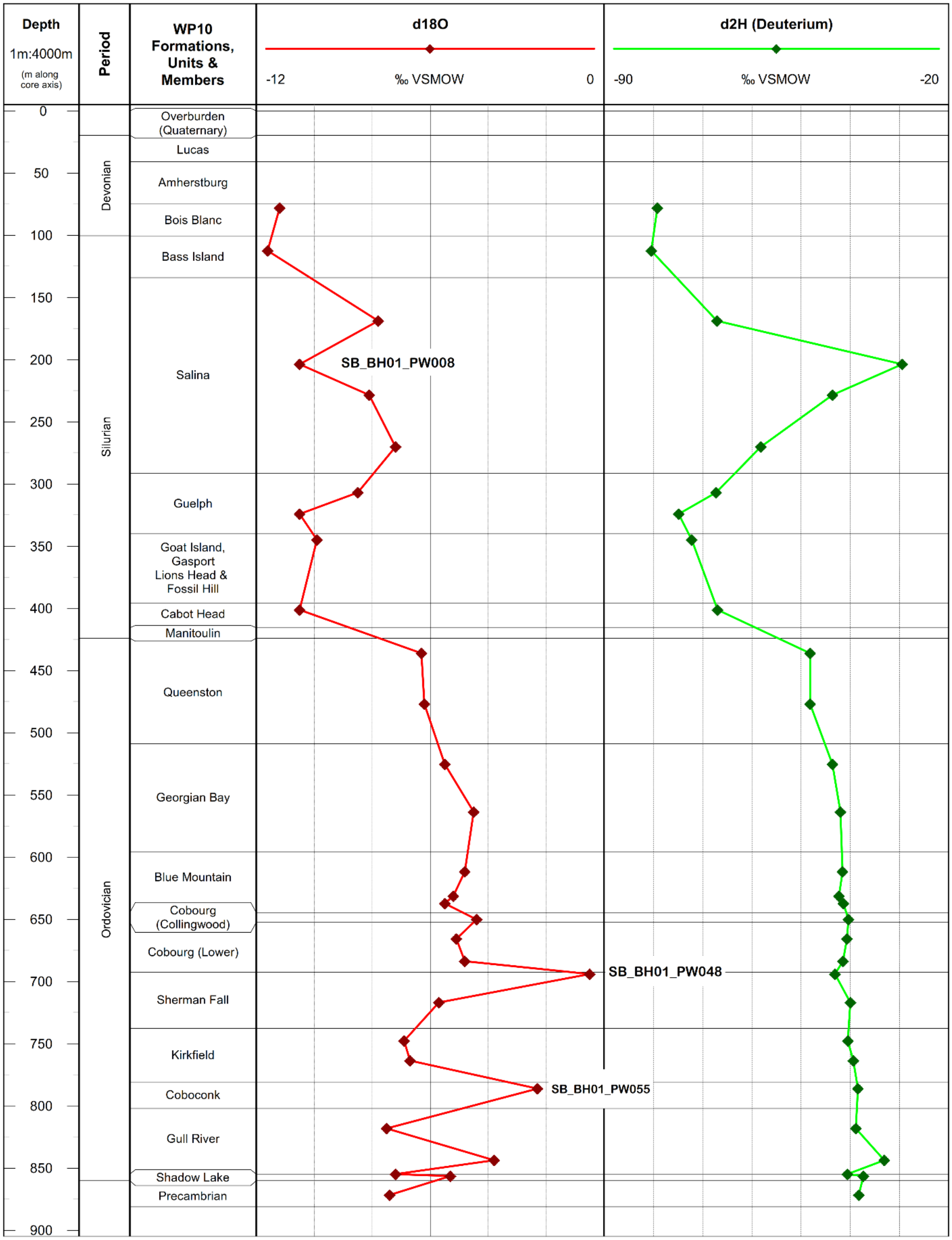

Figure 7 **Profile of $\delta^{18}O$ and $\delta^{2}H$ (Deuterium) of Porewater, SB_BH01 Core Samples.** Samples SB_BH01_PW048 and SB_BH01_PW055 were noted to have low water content (<0.1% and 0.2%, respectively). Subsamples of SB_BH01 PW055 were combined to have sufficient volume for analysis.

3.1.3 Radiohalides and Strontium Isotopes

Figure 8 shows depth profiles for radiohalides (^{129}I, ^{36}Cl, ^{37}Cl) and strontium isotopes ($^{87}Sr/^{86}Sr$) measured from porewater samples at SB_BH01. The porewater that was analyzed was extracted by crushing and leaching fresh core, except for Sr, where both crush and leach and PA methods were used.

The depth profile of the $^{36}Cl/Cl$ (Figure 8) shows decreasing proportions of ^{36}Cl from the top of bedrock to the bottom of the Salina Group and the top of the Guelph Formation, where the lowest ratios are observed (~8.5-8.9 x10^{-16}). From the top of the Guelph Formation, proportions of ^{36}Cl increase rapidly to 3.5x10^{-15} near the top of the Goat Island Formation, and then gradually increase with depth to approximately 6x10^{-15} in Georgian Bay and Blue Mountain formations. Below the Ordovician shales, proportions of ^{36}Cl decrease with depth to the bottom of the Gull River Formation, and then rapidly increase in the Shadow Lake Formation and Precambrian basement rocks.

The depth profile for ^{129}I (Figure 8) shows significant scatter in ^{129}I concentrations for porewaters from the shallow bedrock units up to Cabot Head Formation at approximately 401 m. In these shallow samples, ^{129}I concentrations vary from below detection limits at ~112 m depth to over 5x10^{6} atoms/kgw in the Guelph Formation. From the Cabot Head formation through to the bottom of the Ordovician shales, ^{129}I concentrations are relatively stable between 3.4x10^{5} to 1.4x10^{6} atoms/kgw. In the Ordovician limestones ^{129}I concentrations are an order of magnitude lower than in the overlying shale units and show some scatter between 1.8x10^{4} to 2.6x10^{5}. An anomalous result was recorded for a sample from the Sherman Fall (SB_BH01_PW048) which had a relatively low ^{129}I concentration of 2.8x10^{3} atoms/kgw.

Strontium isotope ratios of $^{87}Sr/^{86}Sr$ were recorded for porewater extracted by both the VDL and PA methods. The PA-derived $^{87}Sr/^{86}Sr$ profile (Figure 8) shows gradually increasing proportions of ^{87}Sr through the Devonian and Silurian strata until stabilizing near a ratio of 0.71 across all the Ordovician-aged strata. In contrast, the VDL-derived $^{87}Sr/^{86}Sr$ profile shows more vertical zonation with sharp changes in the proportion of Sr isotopes near the top of the Cabot Head Formation, at the base of the Ordovician shales, and at the contact with the Precambrian basement rocks. The PA and VDL-derived Sr ratios are similar in the Ordovician shales. In the Ordovician limestones, the PA-derived values are stable near 0.710, while the VDL-derived values show more scatter and are generally lower (~0.709).

Figure 8 also provides a depth profile of isotopic ratios of $\delta^{37}C$ for porewater extracted from core samples. There is significant scatter in $\delta^{37}C$ ratios for samples from the Devonian and Silurian-aged strata, with ratios ranging from -0.91 to +0.58. Except for the sample from the top of the Sherman Fall (SB_BH01_PW048) samples from the Ordovician strata had positive $\delta^{37}C$ ratios between 0-0.5. $\delta^{37}C$ ratios in the Ordovician strata generally decrease from 0.44 near the top of the Queenston Formation to near 0.1 in the Coboconk and Gull River formations. The four deepest samples from the Gull River, Shadow Lake, and Precambrian units show slightly enriched $\delta^{37}C$ compared to samples from the overlying Ordovician limestones.

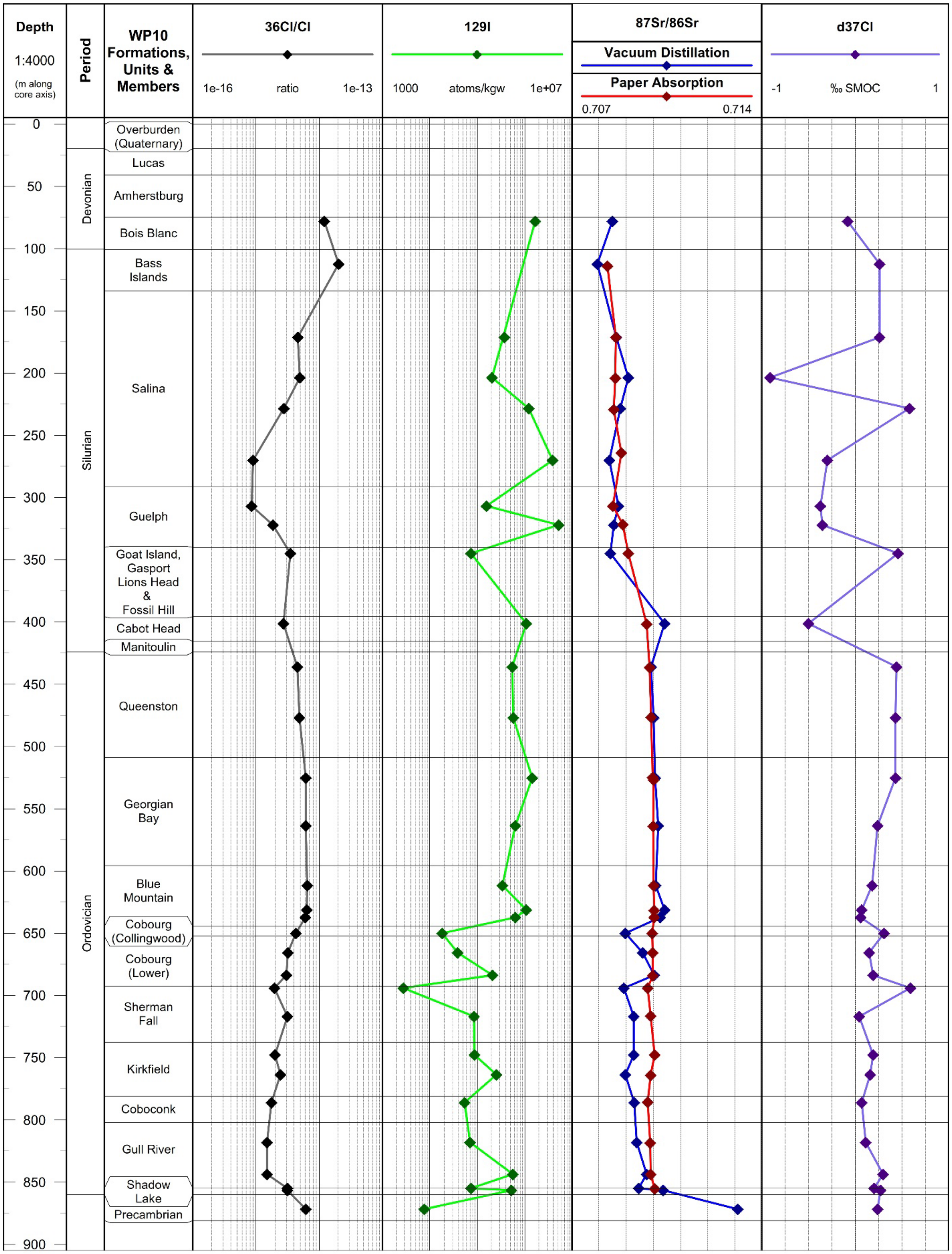

Figure 8 Profile of ^{36}Cl, ^{129}I, $^{87}Sr/^{86}Sr$, and ^{37}Cl Isotopic Results for Porewater from SB_BH01 Core Samples

3.1.4 Noble Gas Concentrations and Isotopes

Figure 9 provides depth profiles of concentrations and isotopic ratios for select noble gases in porewater samples from SB_BH01. Concentrations of He, Ar, and Ne are reported in cubic centimeters of gas per cubic centimeter of water (cc/ccw). Concentrations of Kr were also measured but are not shown in Figure 9. With a few exceptions, concentrations of He, Ar, and Ne in porewaters generally increase with depth, with the highest concentrations observed in the Ordovician strata spanning from the Georgian Bay Formation to the Shadow Lake Formation.

Results from a subset of the noble gas samples show some evidence of atmospheric contamination. The most impacted sample was SB_BH01_NG016, which was collected near middle of the Georgian Bay Formation. Results for SB_BH01_NG016 indicate significant air contamination, with an air-normalized $^{3}He/^{4}He$ ratio of 0.76. Small amounts of air/drill water contamination are expected due to the sampling method, so further assessment of contamination for each NG sample should be completed as part of subsequent data integration activities (WP10).

A depth profile of air-normalized $^{3}He/^{4}He$ ratios (xRa) shows three distinct intervals with similar isotopic ratios of He. Samples from the Bois Blanc and Bass Island have xRa values that are equivalent to or slightly enriched in ^{3}He relative to air. Samples from the Salina Group to the top of the Sherman Fall Formation have xRa ratios between 0.023-0.045. There is an inflection in the xRa profile around 725 m, below which xRa ratios were between 0.051-0.067.

$^{40}Ar/^{36}Ar$ ratios were relatively low (270-390) from the top of rock, through the Devonian and Silurian-aged strata, to the Georgian Bay Formation, except for two samples from the Queenston, that were somewhat enriched in ^{40}Ar with $^{40}Ar/^{36}Ar$ ratios (560-700). Samples from the Blue Mountain and Cobourg formations had $^{40}Ar/^{36}Ar$ ratios between 820-980, that were somewhat higher than samples from the overlying and underlying strata. The highest $^{40}Ar/^{36}Ar$ ratios were measured on porewater from the Gull River and Shadow Lake formations, which had ratios between 1400-3300. The $^{40}Ar/^{36}Ar$ for porewater from a sample in the Precambrian was 290.

All of the porewater samples from SB_BH01 had $^{22}Ne/^{20}Ne$ ratios between 0.09 - 0.11.

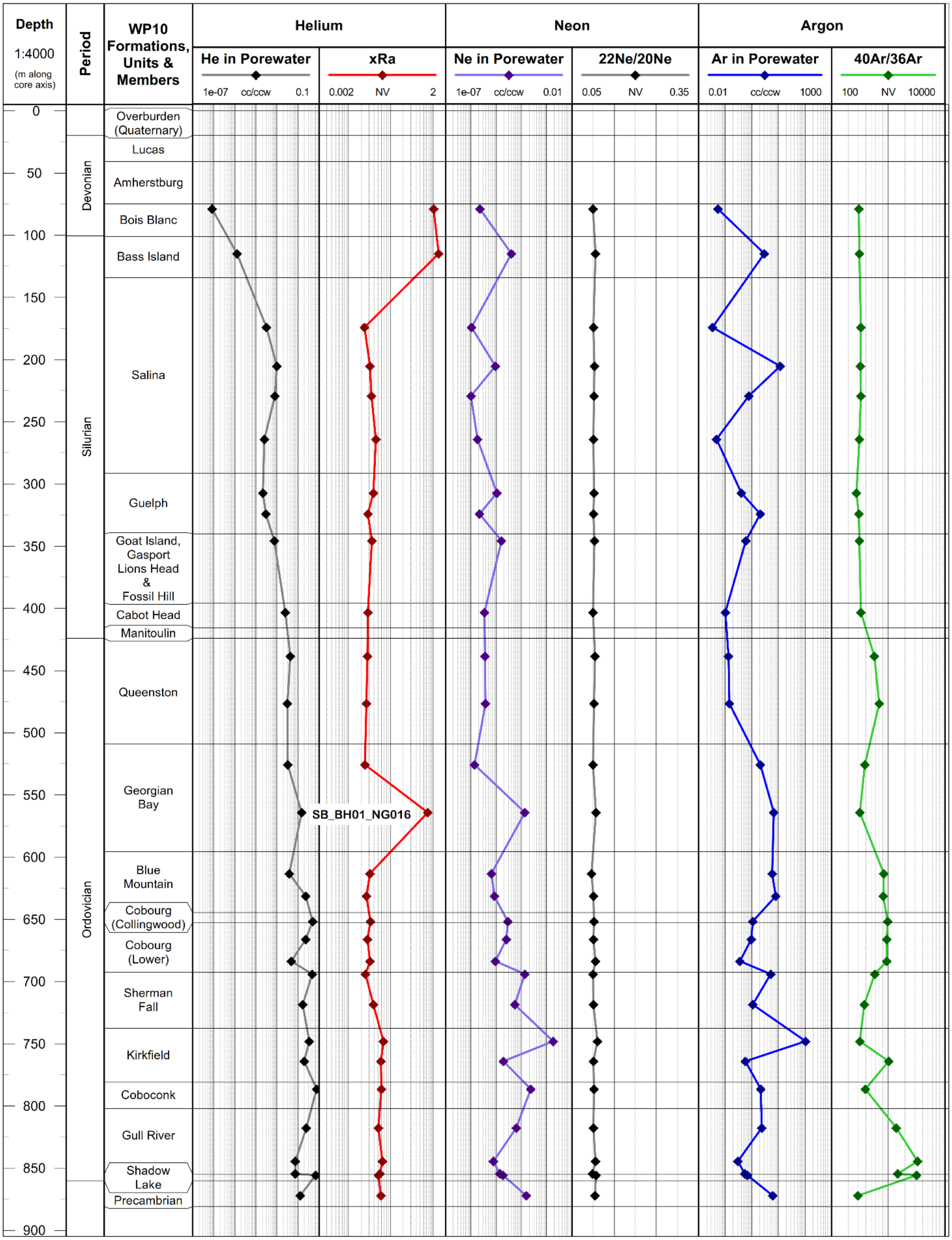

Figure 9 **Profile of Noble Gas (He, Ne, Ar) Concentrations and Isotopes for Porewater from SB_BH01 Core Samples, xRa = Air-normalized $^{3}He/^{4}He$ ratio.**

3.1.5 Methane (CH_4) and Carbon Dioxide (CO_2) Concentrations and Isotopes

Figure 10 shows depths profiles of methane (CH_4) and carbon dioxide (CO_2) concentrations (in mmol/kgw) measured from degassing of core samples into the headspace of Isojars. Concentrations of CH_4 increased with depth from non-detects in the shallow bedrock to approximately 30 mmol/kgw in the Collingwood member of the Cobourg Formation. The highest concentrations of both CO_2 and CH_4 were reported for a sample near the top of the Sherman Fall Formation (SB_BH01_PW048) that had significant degassing observed at the time of sampling, and which has very low water content. Below the Collingwood member of the Cobourg Formation, CH_4 concentrations were around 10 mmol/kgw in samples from the Cobourg (lower), Sherman Fall, and Kirkfield formations.

The profile of $\delta^{13}C$ in CH_4 shows a relative enrichment in ^{13}C with depth from approximately -50 ‰ VPDB in samples from the Salina Group to -40 ‰ VPDB in samples from below the Sherman Fall Formation. The profile of $\delta^{2}H$ for CH_4 also shows an enrichment in ^{2}H from approximately -250 ‰ VSMOW in samples from the Blue Mountain to -180 ‰ VSMOW in samples from the Gull River and Shadow Lake formations.

CO_2 concentrations have a more sporadic profile than CH_4 results, with highly variable concentrations in the shallow bedrock to the Cabot Head Formation. Below the Cabot Head Formation, CO_2concentrations increased gradually to approximately 1.5 mmol/kgw midway through the Blue Mountain Formation. A sharp inflection occurs at the bottom of the Blue Mountain, with lower concentrations of CO_2 in the underlying Cobourg Formation. From the Sherman falls, CO_2 concentrations decrease slightly from around 1.5 mmol/kgw to 0.5 mmol/kgw.

The profile of $\delta^{13}C$ in CO_2 shows a relatively stable depth profile with ratios between -3 to -8 ‰ VPDB. Notable deviations from this range are observed in samples from the top of the Salina Group (-16 ‰ VPDB), the Blue Mountain Formation (+5.2 to 5.7 ‰ VPDB), and the Sherman Fall Formation (+3.5 ‰ VPDB).

3.1 Mineralogy and Petrography

Mineralogical and petrographic analyses were completed to obtain sample-specific mineralogical data required for interpretation of the porewater results and reconstructive geochemical modelling. This advanced analyses of porewater results will be completed as part of data integration (WP10) activities, so results from the mineralogical and petrographic testing are not discussed in detail in this data report. The mineralogical testing completed as part of this work package (WP04C) complements more substantial mineralogical testing program that was completed by SGS Laboratories and the British Geologic Survey as part of WP04D.

Figure 11 shows the major mineralogical components (by XRD) for core porewater (PW) samples that were also used for the PA method. Shale samples from the Cabot Head, Queenston, Georgian Bay, and Blue Mountain formations show a variable mineralogy, including significant proportions of clay minerals and quartz. Calcite is the most abundant mineral in samples from the Ordovician limestones, except for the porous dolomite-dominated sample from near the top of the Sherman Fall. The sample from the Shadow Lake shows similar proportions of quartz and clay minerals, consistent with a logged lithology of a silty/shaley sandstone.

Complete results from the mineralogical and petrographic analyses are provided in Appendix C.

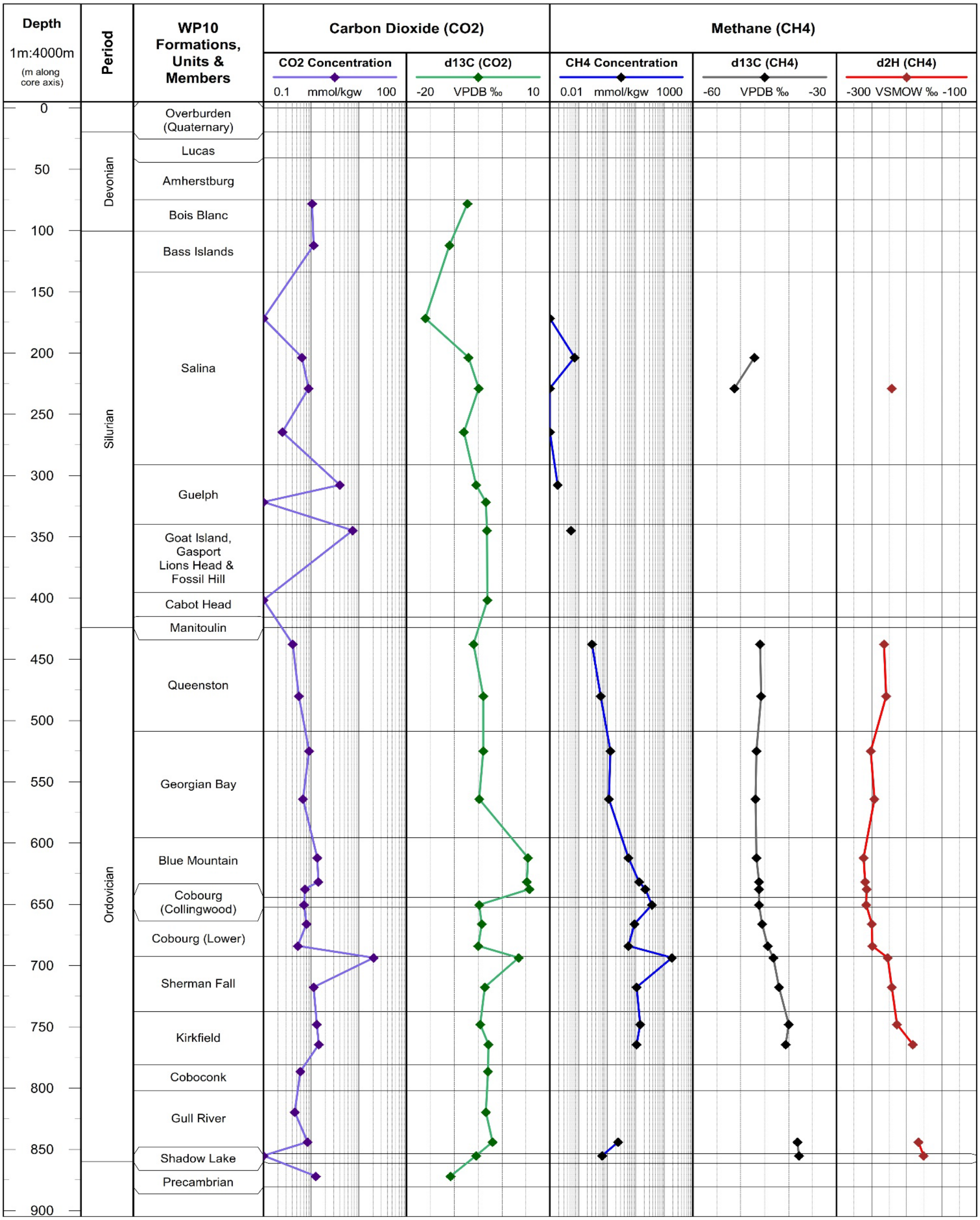

Figure 10 **Profile of Methane and Carbon Dioxide Concentrations and Isotopes from SB_BH01 Core Samples**

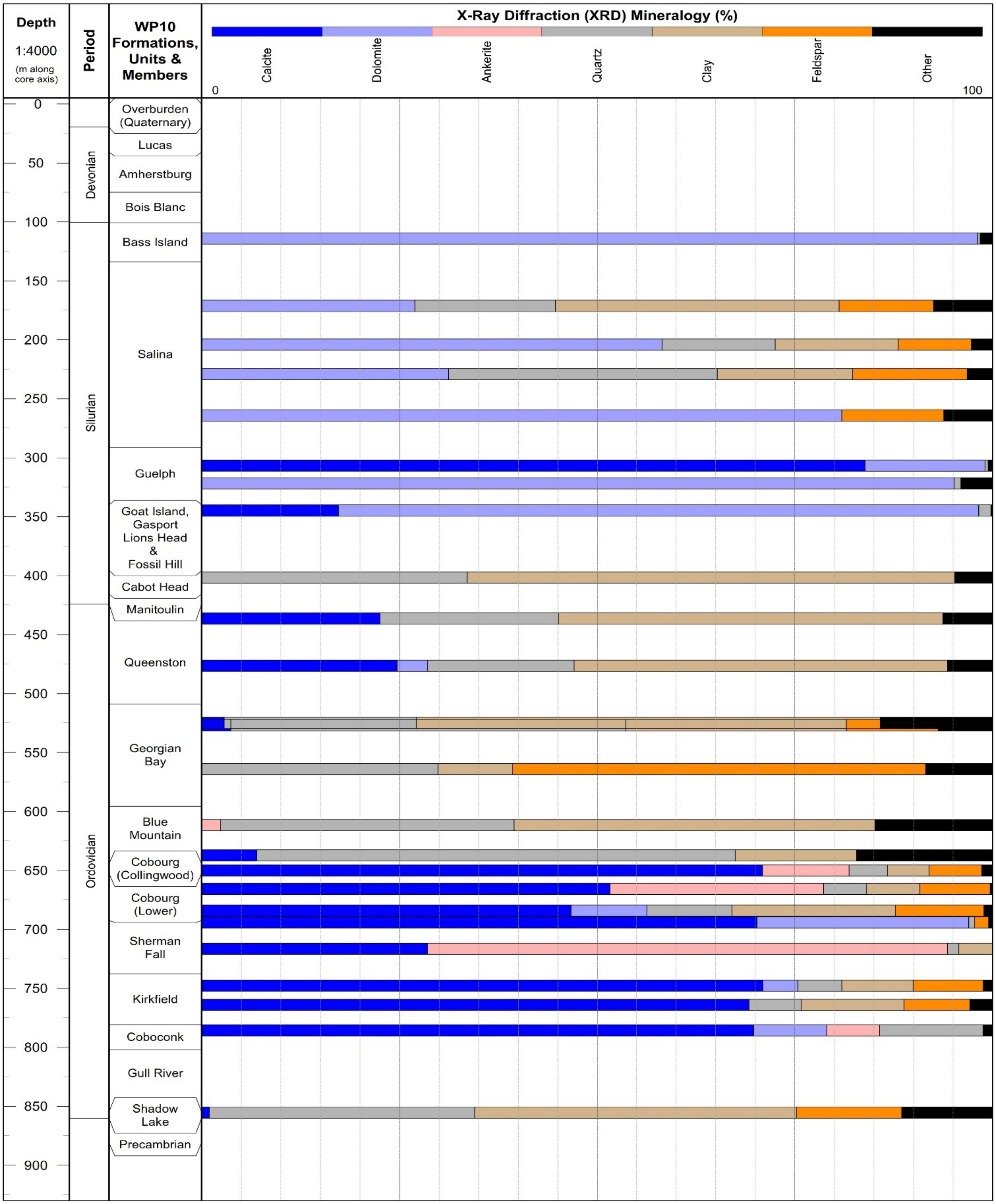

Figure 11 Mineralogical Components, by X-Ray Diffraction, SB_BH01 Core Samples

4 CONCLUSIONS

Geofirma Engineering Ltd. completed sampling and preservation of core samples as part of porewater characterization activities (Work Package 04C) at SB_BH01, the first of two boreholes in the South Bruce site that were drilled as part of the NWMO's Phase 2 Geoscientific Preliminary Field Investigations. The porewater samples were collected and preserved between June 1 to September 16, 2021.

A total of 121 preserved samples were sent to the University of Ottawa for analysis, including:

- 30 pairs of porewater (PW) samples for porewater analysis. Each pair included one PW sample that was used for vacuum distillation leaching (VDL), and a second PW sample that was used for paper absorption (PA) and mineralogical analyses.
- 2 archive (AR) samples as replacements for PW samples that were damaged in transit from the drill site to the laboratory.
- 29 dissolved gas (DG) samples collected in IsoJars™ for measurement of carbon dioxide and methane concentrations and their associated isotopic ratios (δ^2H, $\delta^{13}C$).
- 30 noble gas (NG) samples that were encapsulated in air-tight stainless-steel vessels for measurement of noble gas concentrations and isotopic compositions.

Porewater extraction and laboratory testing completed as part of porewater characterization activities for SB_BH01, including the accompanying mineralogical and petrographic testing, was coordinated by the University of Ottawa, with a subset of analyses completed by subcontracted research and commercial laboratories.

Results from the porewater characterization program provide high resolution depth profiles of key porewater parameters, including major/minor ionic composition, environmental isotopes, radiohalides, dissolved gases, and noble gases. Results presented in this report show laboratory-reported values, but were not corrected for mineral dissolution, halite under-saturation, and anion exclusion processes. Detailed interpretation of the porewater results, including geochemical modelling, will be completed separately as part of data integration activities (Work Package 10).

Notable results from the porewater characterization program at SB_BH01 include:

- Comparison of Cl and Na concentrations measured using the VDL and PA methods show substantial variation, with PA-derived concentrations that were 1-3 orders of magnitude higher than corresponding concentrations obtained using the VDL method. The variation may reflect differences in the proportional uptake of clay-bound, capillary-bound, and mobile porewaters.
- Na and Cl dominate the ionic composition of porewaters, particularly below the Salina Group.
- TDS concentrations calculated assuming a water density of 1000 kg/m^3 were below 10 g/L in the Devonian units, between 18-111 g/L in the Salina Group and Guelph Formation and increased values through the lower Silurian and Ordovician aged strata to approximately 250-350 g/L below the Georgian Bay Formation.

- Profiles for environmental isotopes (^{18}O, ^{2}H), radiohalides (^{36}Cl, ^{129}I) and $^{87}Sr/^{86}Sr$ in porewater consistently show variation in isotopic ratios with depth across the Paleozoic bedrock sequence. Inflections were generally observed in the depth profiles for these analytes near the top of the Salina Group, near the top of the Ordovician shales (Queenston Formation), and near the top of the Ordovician carbonates (Cobourg Fm).

- A profile of air-normalized $^{3}He/^{4}He$ ratios (xRa) shows three distinct depth intervals with similar He isotopic ratios. Samples from the Bois Blanc and Bass Island have xRa values that are equivalent to or slightly enriched in ^{3}He relative to air, while samples from the Salina Group to the top of the Sherman Fall Formation have xRa ratios between 0.023-0.045. There is an inflection in the xRa profile around 725 m, below which xRa ratios were between 0.051-0.067

- Methane concentrations generally increased with depth, with the highest concentrations observed from samples near the top of the Cobourg Formation and the top of the Sherman Fall Formation. Profiles of $\delta^{13}C$ and $\delta^{2}H$ in methane show relative enrichment of both isotopes with depth.

5 REFERENCES

Altinier, M.V., S. Savoye, J.-L. Michelot, C. Beaucaire, M. Massault, D. Tessier and N.H. Waber, 2007. The isotopic composition of pore-water from Tournemire argillite (France): An inter-comparison study. Physics and Chemistry of the Earth, Vol. 32, pp. 209-218.

Armstrong, D.K. and Carter T.R, 2010. Special volume 7: the Subsurface Paleozoic Stratigraphy of Southern Ontario (Open file report, 0826-9580; 6191). Ministry of Energy, Northern Development and Mines

Clark, I.D., T. Al, M. Jensen, L. Kennell, M. Mazurek, R. Mohapatra and K.G. Raven, 2013. Paleozoic-aged brine and authigenic helium preserved in an Ordovician shale aquiclude. Geology, Vol. 41, pp. 951-954

Celejewski, M, D. Barton and T. Al, 2018. Measurement of Cl–Br ratios in porewater of clay rich rocks – A comparison of the crush and leach and paper absorption methods, Geofluids, Special Issue on Aquitard Fluids and Gases.

Celejewski, M. L. Scott and T. Al, 2014. An absorption method for extraction and characterization of porewater from low-permeability rocks using cellulosic sheets. Applied Geochemistry, Vol. 49, pp. 22-30

Geofirma Engineering Ltd. 2022. WP03 Data Report: Geological and Geotechnical Core Logging, Photography, and Sampling for SB_BH01, Phase 2 Initial Borehole Drilling and Testing, South Bruce. Prepared for: Nuclear Waste Management Organization, Toronto, Ontario. Revision 0.

Intera Engineering Ltd., 2011. Descriptive Geosphere Site Model, OPG's Deep Geologic Repository for Low & Intermediate Level Waste, Report NWMO DGR-TR-2011-24, March.

Appendix A

SB_BH01 Porewater (PW), Dissolved Gas (DG), and Noble Gas (NG) Sample Summary

Sample ID	Sample Type	From (m)	To (m)	Date Sampled	Lithology	Comments
SB_BH01_AR001	AR	43.93	44.17	2021-06-01 10:45	Limestone	Shipped to U Ottawa as per NWMO direction for additional analysis as a sanmple set with SB_BH01_PW001
SB_BH01_AR013	AR	270.12	270.43	2021-07-20 14:39	Dolostone	Analyzed in the place of SB_BH01_PW012, which was damaged during transport to U Ottawa
SB_BH01_AR034	AR	638.64	638.88	2021-08-27 21:06	Shale	
SB_BH01_DG001	DG	78.13	78.23	2021-06-15 21:00	Limestone	
SB_BH01_DG002	DG	112.05	112.15	2021-06-20 3:30	Dolostone	
SB_BH01_DG004	DG	168.56	168.66	2021-07-17 3:00	Shale	Top and bottom depth updated (21-Sep-23) as part of CAR23-008
SB_BH01_DG005	DG	203.57	203.71	2021-07-18 9:55	Shale	
SB_BH01_DG006	DG	228.93	229.07	2021-07-19 18:21	Anhydrite	
SB_BH01_DG007	DG	264.52	264.64	2021-07-20 13:26	Dolostone	
SB_BH01_DG008	DG	307.6	307.7	2021-07-31 5:43	Limestone	
SB_BH01_DG009	DG	324.49	324.59	2021-08-02 15:40	Dolostone	Top and bottom depth updated (21-Sep-23) as part of CAR23-008
SB_BH01_DG010	DG	345.09	345.19	2021-08-03 6:52	Limestone	
SB_BH01_DG012	DG	401.82	401.95	2021-08-07 22:15	Shale	
SB_BH01_DG013	DG	437.76	437.9	2021-08-10 12:15	Shale	
SB_BH01_DG014	DG	480.02	480.13	2021-08-13 3:40	Shale	Green calcareous shale
SB_BH01_DG015	DG	524.92	525.02	2021-08-15 11:00	Shale	
SB_BH01_DG016	DG	563.96	564.06	2021-08-18 10:45	Shale	Shale interbedded with hard carbonate (calcareous) sand and minor limestone
SB_BH01_DG017	DG	612.24	612.34	2021-08-26 2:31	Shale	
SB_BH01_DG018	DG	631.85	631.95	2021-08-27 8:35	Shale	
SB_BH01_DG019	DG	637.72	637.82	2021-08-27 13:14	Shale	Originally archived, submitted to U Ottawa on Nov 3, 2021
SB_BH01_DG020	DG	650.43	650.55	2021-08-28 1:37	Limestone	
SB_BH01_DG021	DG	666.11	666.22	2021-08-29 12:08	Limestone	
SB_BH01_DG022	DG	684.14	684.25	2021-08-30 2:41	Limestone	
SB_BH01_DG024	DG	693.82	693.93	2021-08-30 14:00	Limestone	Extra time sensitive suite from degassing coarse grained limestone
SB_BH01_DG025	DG	717.66	717.77	2021-09-02 16:06	Limestone	
SB_BH01_DG026	DG	748.16	748.26	2021-09-09 17:25	Limestone	
SB_BH01_DG027	DG	764.37	764.48	2021-09-11 2:45	Limestone	Hard limestone and shales
SB_BH01_DG028	DG	786.35	786.49	2021-09-12 12:29	Limestone	
SB_BH01_DG029	DG	819.6	819.7	2021-09-13 23:30	Limestone	
SB_BH01_DG030	DG	844.03	844.14	2021-09-14 17:35	Limestone	Sample contains intact natural fracture with gypsum infill
SB_BH01_DG032	DG	855.19	855.29	2021-09-15 17:13	Sandstone	Glauconitic sandstone; Shadow Lake sample suite
SB_BH01_DG033	DG	872.22	872.35	2021-09-16 17:28	Gneiss	
SB_BH01_NG001	NG	78.82	78.92	2021-06-15 21:30	Limestone	
SB_BH01_NG002	NG	114.88	114.99	2021-06-20 5:30	Dolostone	
SB_BH01_NG004	NG	174.21	174.34	2021-07-17 4:40	Dolostone	Top and bottom depth updated (21-Sep-23/18-Dec-23) as part of CAR23-008
SB_BH01_NG005	NG	205.13	205.27	2021-07-18 13:20	Dolostone	
SB_BH01_NG006	NG	229.13	229.27	2021-07-19 16:35	Shale	
SB_BH01_NG007	NG	264.14	264.3	2021-07-20 11:19	Dolostone	
SB_BH01_NG008	NG	307.47	307.6	2021-07-31 5:38	Limestone	
SB_BH01_NG009	NG	324.1	324.24	2021-08-02 15:45	Dolostone	Top and bottom depth updated (21-Sep-23) as part of CAR23-008
SB_BH01_NG010	NG	345.75	345.86	2021-08-03 11:40	Limestone	
SB_BH01_NG012	NG	403.33	403.45	2021-08-08 2:50	Shale	
SB_BH01_NG013	NG	438.42	438.54	2021-08-10 12:10	Shale	
SB_BH01_NG014	NG	476.59	476.72	2021-08-12 14:50	Shale	
SB_BH01_NG015	NG	525.93	526.05	2021-08-15 14:30	Shale	
SB_BH01_NG016	NG	564.06	564.17	2021-08-18 10:45	Shale	Hard Shale interbedded with carbonate(calcareous) sand and limestone.
SB_BH01_NG017	NG	613.42	613.55	2021-08-26 6:07	Shale	
SB_BH01_NG018	NG	631.3	631.43	2021-08-27 8:30	Shale	
SB_BH01_NG020	NG	651.89	652	2021-08-28 5:06	Limestone	
SB_BH01_NG021	NG	665.97	666.11	2021-08-29 12:08	Limestone	
SB_BH01_NG022	NG	683.59	683.71	2021-08-30 2:41	Limestone	
SB_BH01_NG024	NG	694.32	694.43	2021-08-30 14:00	Limestone	Extra time sensitive suite from degassing coarse grained limestone.
SB_BH01_NG025	NG	718.43	718.57	2021-09-02 16:25	Limestone	
SB_BH01_NG026	NG	748.02	748.16	2021-09-09 17:40	Limestone	
SB_BH01_NG027	NG	764.19	764.32	2021-09-11 2:30	Limestone	Limestone with hard shale layers
SB_BH01_NG028	NG	786.6	786.7	2021-09-12 14:01	Limestone	
SB_BH01_NG029	NG	817.6	817.7	2021-09-13 20:45	Limestone	
SB_BH01_NG030	NG	844.23	845.35	2021-09-14 17:59	Limestone	Sample not weighed prior to preservation.
SB_BH01_NG031	NG	852.34	852.45	2021-09-15 6:06	Shale	Conservative early collection of possible Shadow Lake Fm
SB_BH01_NG032	NG	854.71	854.86	2021-09-15 9:05	Sandstone	Weakly glauconitic sand; recollected as NG033
SB_BH01_NG033	NG	855.9	856.06	2021-09-15 11:25	Sandstone	Glauconitic sandstone; Shadow Lake sample suite
SB_BH01_NG034	NG	872.11	872.22	2021-09-16 17:28	Gneiss	
SB_BH01_PW001	PW-VD	78.23	78.47	2021-06-15 21:00	Limestone	
SB_BH01_PW002	PW-VD	112.61	112.85	2021-06-20 3:30	Dolostone	
SB_BH01_PW003	PW-PA	114.08	114.27	2021-06-20 3:30	Dolostone	
SB_BH01_PW006	PW-VD	168.9	169.08	2021-07-17 3:00	Shale	Top and bottom depth updated (21-Sep-23) as part of CAR23-008
SB_BH01_PW007	PW-PA	168.66	168.9	2021-07-17 3:00	Shale	Top and bottom depth updated (21-Sep-23) as part of CAR23-008
SB_BH01_PW008	PW-VD	203.71	203.95	2021-07-18 9:38	Shale	
SB_BH01_PW009	PW-PA	203.95	204.23	2021-07-18 9:45	Shale	
SB_BH01_PW010	PW-VD	228.59	228.88	2021-07-19 16:05	Shale	
SB_BH01_PW011	PW-PA	229.27	229.58	2021-07-19 16:20	Shale	
SB_BH01_PW012	PW-VD	264.3	264.5	2021-07-20 11:04	Dolostone	Package damaged upon receipt at U Ottawa, alternative sample shipped as a replacment (SB_BH01_AR013)
SB_BH01_PW013	PW-PA	263.86	264.14	2021-07-20 10:54	Dolostone	
SB_BH01_PW014	PW-VD	306.77	307.02	2021-07-31 5:40	Limestone	
SB_BH01_PW015	PW-PA	307.02	307.17	2021-07-31 5:40	Limestone	

Sample ID	Sample Type	From (m)	To (m)	Date Sampled	Lithology	Comments
SB_BH01_PW016	PW-VD	323.9	324.1	2021-08-02 15:38	Dolostone	Top and bottom depth updated (21-Sep-23) as part of CAR23-008
SB_BH01_PW017	PW-PA	324.24	324.49	2021-08-02 15:40	Dolostone	Top and bottom depth updated (21-Sep-23) as part of CAR23-008
SB_BH01_PW018	PW-VD	344.74	344.89	2021-08-03 6:49	Limestone	
SB_BH01_PW019	PW-PA	344.89	345.09	2021-08-03 6:50	Limestone	
SB_BH01_PW022	PW-VD	401.25	401.48	2021-08-07 22:25	Shale	
SB_BH01_PW023	PW-PA	401.48	401.82	2021-08-07 22:10	Shale	
SB_BH01_PW024	PW-VD	436.15	436.33	2021-08-10 11:50	Shale	
SB_BH01_PW025	PW-PA	436.33	436.59	2021-08-10 12:04	Shale	
SB_BH01_PW026	PW-PA	476.28	476.59	2021-08-12 14:50	Shale	
SB_BH01_PW027	PW-VD	476.75	476.92	2021-08-12 14:50	Shale	
SB_BH01_PW028	PW-PA	525.17	525.36	2021-08-15 11:00	Shale	
SB_BH01_PW029	PW-VD	524.71	524.92	2021-08-15 11:00	Shale	Shale sample broke into 2 pieces during collection and preservation
SB_BH01_PW030	PW-PA	526.8	527.06	2021-08-15 14:30	Shale	Alternative to PW029 which was damaged during sampling
SB_BH01_PW031	PW-VD	563.76	563.96	2021-08-18 10:35	Shale	Hard Shale interbedded with carbonate(calcareous) sand and limestone
SB_BH01_PW032	PW-PA	564.17	564.43	2021-08-18 13:35	Shale	Hard Shale interbedded with carbonate(calcareous) sand and limestone.
SB_BH01_PW033	PW-VD	611.86	612.08	2021-08-26 2:27	Shale	
SB_BH01_PW034	PW-PA	611.64	611.86	2021-08-26 2:30	Shale	
SB_BH01_PW035	PW-VD	631.43	631.61	2021-08-27 8:30	Shale	
SB_BH01_PW036	PW-PA	631.61	631.85	2021-08-27 8:35	Shale	
SB_BH01_PW037	PW-VD	637.18	637.33	2021-08-27 13:10	Shale	Originally archived as per NWMO request, shipped to U Ottawa for Analysis on Nov 3
SB_BH01_PW038	PW-PA	637.33	637.54	2021-08-27 13:13	Shale	Originally archived as per NWMO request, shipped to U Ottawa for Analysis on Nov 3
SB_BH01_PW039	PW-VD	650.25	650.43	2021-08-28 1:47	Limestone	
SB_BH01_PW040	PW-PA	650.02	650.25	2021-08-28 1:48	Limestone	
SB_BH01_PW041	PW-PA	665.53	665.75	2021-08-29 12:08	Limestone	
SB_BH01_PW042	PW-VD	665.75	665.97	2021-08-29 12:08	Limestone	
SB_BH01_PW043	PW-VD	683.71	683.87	2021-08-30 2:40	Limestone	
SB_BH01_PW044	PW-PA	683.87	684.14	2021-08-30 2:40	Limestone	
SB_BH01_PW047	PW-VD	693.93	694.12	2021-08-30 14:00	Limestone	Extra time sensitive suite from degassing coarse grained limestone.
SB_BH01_PW048	PW-PA	694.12	694.32	2021-08-30 14:00	Limestone	Extra time sensitive suite from degassing coarse grained limestone.
SB_BH01_PW049	PW-PA	716.6	716.81	2021-09-02 10:00	Limestone	
SB_BH01_PW050	PW-VD	716.81	716.99	2021-09-02 10:00	Limestone	
SB_BH01_PW051	PW-VD	747.58	747.75	2021-09-09 15:15	Limestone	
SB_BH01_PW052	PW-PA	747.75	748.02	2021-09-09 17:19	Limestone	
SB_BH01_PW053	PW-VD	763.64	763.8	2021-09-11 2:30	Limestone	limestone with shale interbeds
SB_BH01_PW054	PW-PA	763.96	764.19	2021-09-11 2:36	Limestone	
SB_BH01_PW055	PW-VD	786.12	786.35	2021-09-12 12:25	Limestone	
SB_BH01_PW056	PW-PA	785.86	786.12	2021-09-12 12:28	Limestone	
SB_BH01_PW057	PW-VD	818.05	818.26	2021-09-13 20:45	Limestone	
SB_BH01_PW058	PW-PA	818.26	818.58	2021-09-13 20:50	Limestone	
SB_BH01_PW059	PW-VD	843.6	843.78	2021-09-14 17:20	Limestone	
SB_BH01_PW060	PW-PA	843.78	844.03	2021-09-14 17:25	Limestone	Sample contains intact natural fracture with gypsum infill
SB_BH01_PW063	PW-PA	855.29	855.5	2021-09-15 8:58	Sandstone	Glauconitic sandstone; "Porewater 2" of Shadow Lake sample suite
SB_BH01_PW064	PW-VD	855.03	855.18	2021-09-15 8:58	Sandstone	Contains transition from weakly glauconitic sand to strongly glauconitic sand at 855.18; recollected as PW065
SB_BH01_PW065	PW-VD	856.42	856.58	2021-09-15 11:01	Sandstone	Glauconitic sandstone; "Porewater 1" of Shadow Lake sample suite
SB_BH01_PW066	PW-VD	871.7	871.87	2021-09-16 16:27	Gneiss	
SB_BH01_PW067	PW-PA	871.87	872.11	2021-09-16 17:27	Gneiss	

Ar = Archive
DG = Dissolved Gas
NG = Noble Gas
PW-VD = Porewater, Vacuum Distillation Leaching Method
PW-PA = Porewater, Paper Absorption Method

Appendix B

Results Tables for Porewater Characterization Activities at SB_BH01

C.1. – Porewater Sample Results – VDL
C.2 – Porewater Sample Results – PA
C.3 – Noble Gas Sample Results
C.4. Dissolved Gas Sample Results

Sample ID		SB_BH01_PW001	SB_BH01_PW002	SB_BH01_PW006	SB_BH01_PW008	SB_BH01_PW010	SB_BH01_PW014	SB_BH01_PW016
Major/Minor Ions								
Aluminum (Al)	mmol/kgw	0.03	0.03	0.01	0.09	0.01	0.14	0.02
Boron (B)	mmol/kgw	0.94	0.74	4.27	25.11	3.31	3.55	0.66
Bromine (Br)	mmol/kgw	0.03	0.02	0.44	3.06	1.11	3.78	0.44
Calcium (Ca)	mmol/kgw	26.30	17.39	110.09	75.60	150.42	231.12	32.17
Chlorine (Cl)	mmol/kgw	9.96	5.40	162.54	1142.17	358.83	1442.38	528.42
Iodine (I)	mmol/kgw	0.00	0.00	0.00	0.01	0.00	0.03	0.00
Iron (Fe)	mmol/kgw	0.00	0.00	0.00	0.01	0.02	0.03	0.00
Lithium (Li)	mmol/kgw	0.01	0.01	0.06	0.72	0.11	1.01	0.16
Magnesium (Mg)	mmol/kgw	13.21	13.37	26.61	37.66	29.61	115.42	30.86
Manganese (Mn)	mmol/kgw	0.00	0.00	0.00	0.00	0.00	0.00	0.00
Potassium (K)	mmol/kgw	0.14	0.13	5.77	48.19	4.96	17.57	3.69
Rubidium (Rb)	mmol/kgw	0.00	0.00	0.00	0.01	0.00	0.01	0.00
Silicon (Si)	mmol/kgw	17.43	0.57	6.40	49.67	6.07	65.39	8.89
Sodium (Na)	mmol/kgw	8.56	5.35	132.26	1365.38	187.81	877.16	438.74
Strontium (Sr)	mmol/kgw	0.33	3.62	0.61	0.40	1.20	3.78	0.33
Sulfur (S)	mmol/kgw	40.80	35.48	132.24	255.11	111.56	112.52	40.72
Environmental Isotopes								
$\delta^{18}O$	‰VSMOW	-11.2	-11.6	-7.8	-10.5	-8.1	-8.5	-10.5
$\delta^{2}H$	‰VSMOW	-79.2	-80.4	-67.1	-29.5	-43.6	-67.3	-74.8
Radiohalides and Strontium Isotopes								
Chlorine-37 ($\delta^{37}Cl$)	‰ SMOC	-0.08	0.26	0.26	-0.91	0.58	-0.37	-0.35
Chlorine-36 ($^{36}Cl/Cl$)	--	1.19E-14	2.03E-14	4.56E-15	4.96E-15	2.75E-15	8.54E-16	1.84E-15
Iodine-129 (^{129}I)	atoms/kgw	1.69E+00	BDL	3.72E-01	2.03E-01	1.21E+00	1.56E-01	5.23E+00
Strontium isotope ratio ($^{87}Sr/^{86}Sr$)	--	0.70849	0.70794	0.70864	0.70907	0.70878	0.70870	0.70854
BDL = Below Detection Limit								

Sample ID		SB_BH01_PW018	SB_BH01_PW022	SB_BH01_PW024	SB_BH01_PW027	SB_BH01_PW028	SB_BH01_PW031	SB_BH01_PW034
Major/Minor Ions								
Aluminum (Al)	mmol/kgw	0.19	0.05	0.02	0.03	0.03	0.02	0.03
Boron (B)	mmol/kgw	10.61	6.30	6.93	5.71	5.41	6.07	4.99
Bromine (Br)	mmol/kgw	3.54	2.73	15.82	17.79	19.76	23.08	20.11
Calcium (Ca)	mmol/kgw	138.94	148.83	584.64	648.16	681.63	874.92	748.59
Chlorine (Cl)	mmol/kgw	2526.73	2528.57	3912.65	4275.10	4749.18	5387.32	4941.70
Iodine (I)	mmol/kgw	0.03	0.01	0.04	0.06	0.07	0.07	0.06
Iron (Fe)	mmol/kgw	0.03	0.02	0.00	0.00	0.02	0.01	0.00
Lithium (Li)	mmol/kgw	0.62	0.47	1.09	1.56	1.75	2.18	1.77
Magnesium (Mg)	mmol/kgw	96.20	46.96	252.60	267.33	239.86	257.60	218.72
Manganese (Mn)	mmol/kgw	0.00	0.00	0.05	0.08	0.21	0.29	0.26
Potassium (K)	mmol/kgw	34.39	142.15	228.76	259.26	300.28	311.38	295.69
Rubidium (Rb)	mmol/kgw	0.01	0.03	0.06	0.07	0.08	0.08	0.09
Silicon (Si)	mmol/kgw	92.77	13.28	18.49	18.30	17.69	17.38	18.94
Sodium (Na)	mmol/kgw	2230.70	2032.52	2051.97	2279.80	2548.69	2739.73	2594.43
Strontium (Sr)	mmol/kgw	3.08	1.04	3.73	4.97	5.13	7.04	7.52
Sulfur (S)	mmol/kgw	148.88	22.12	24.15	33.33	9.21	15.83	8.60
Environmental Isotopes								
$\delta^{18}O$	‰VSMOW	-9.9	-10.5	-6.3	-6.2	-5.5	-4.5	-4.8
$\delta^{2}H$	‰VSMOW	-72.2	-67	-48.2	-48.2	-43.6	-42	-41.6
Radiohalides and Strontium Isotopes								
Chlorine-37 ($\delta^{37}Cl$)	‰ SMOC	0.46	-0.50	0.44	0.43	0.43	0.24	0.18
Chlorine-36 ($^{36}Cl/Cl$)	--	3.47E-15	2.70E-15	4.54E-15	4.84E-15	6.10E-15	6.15E-15	6.43E-15
Iodine-129 (^{129}I)	atoms/kgw	7.37E-02	1.08E+00	5.50E-01	5.83E-01	1.44E+00	6.40E-01	3.39E-01
Strontium isotope ratio ($^{87}Sr/^{86}Sr$)	--	0.70842	0.71041	0.70992	0.71001	0.71007	0.71018	0.71008
BDL = Below Detection Limit								

Sample ID		SB_BH01_PW035	SB_BH01_PW037	SB_BH01_PW039	SB_BH01_PW042	SB_BH01_PW043	SB_BH01_PW048	SB_BH01_PW050
Major/Minor Ions								
Aluminum (Al)	mmol/kgw	0.02	0.03	0.21	0.15	0.09	0.38	0.28
Boron (B)	mmol/kgw	4.77	5.00	22.62	19.27	9.78	26.79	20.12
Bromine (Br)	mmol/kgw	18.67	17.19	19.63	20.77	19.03	25.03	20.71
Calcium (Ca)	mmol/kgw	756.32	750.27	849.03	771.38	674.47	1896.54	632.69
Chlorine (Cl)	mmol/kgw	4645.77	4634.35	5260.69	5359.37	4774.21	23700.61	5111.04
Iodine (I)	mmol/kgw	0.05	0.06	0.08	0.07	0.07	0.10	0.08
Iron (Fe)	mmol/kgw	0.01	0.01	0.02	0.08	0.00	0.62	0.01
Lithium (Li)	mmol/kgw	1.14	1.17	3.95	2.58	1.89	2.47	3.08
Magnesium (Mg)	mmol/kgw	176.18	189.43	387.26	369.95	304.24	629.97	341.12
Manganese (Mn)	mmol/kgw	0.19	0.23	0.04	0.03	0.03	0.06	0.01
Potassium (K)	mmol/kgw	253.63	241.49	288.90	259.25	288.32	241.63	270.79
Rubidium (Rb)	mmol/kgw	0.06	0.06	0.10	0.07	0.08	0.05	0.07
Silicon (Si)	mmol/kgw	18.81	19.58	144.26	119.09	59.47	256.03	210.44
Sodium (Na)	mmol/kgw	2562.84	2565.43	2915.90	2790.29	2665.68	19124.43	2859.83
Strontium (Sr)	mmol/kgw	6.34	6.90	12.10	10.23	8.51	25.02	10.23
Sulfur (S)	mmol/kgw	8.18	17.05	432.47	154.45	70.44	946.50	102.79
Environmental Isotopes								
$\delta^{18}O$	‰VSMOW	-5.2	-5.5	-4.4	-5.1	-4.8	-0.5	-5.7
$\delta^{2}H$	‰VSMOW	-42.3	-41.4	-40.4	-40.7	-41.5	-43.1	-40
Radiohalides and Strontium Isotopes								
Chlorine-37 ($\delta^{37}Cl$)	‰ SMOC	0.07	0.06	0.31	0.15	0.19	0.59	0.04
Chlorine-36 ($^{36}Cl/Cl$)	--	6.38E-15	6.05E-15	4.25E-15	3.22E-15	3.04E-15	1.96E-15	3.15E-15
Iodine-129 (^{129}I)	atoms/kgw	1.09E+00	6.40E-01	1.82E-02	3.85E-02	2.10E-01	2.75E-03	8.54E-02
Strontium isotope ratio ($^{87}Sr/^{86}Sr$)	--	0.71041	0.71025	0.70897	0.70961	0.71004	0.70891	0.70927
BDL = Below Detection Limit								

Sample ID		SB_BH01_PW051	SB_BH01_PW053	SB_BH01_PW055	SB_BH01_PW057	SB_BH01_PW059	SB_BH01_PW064	SB_BH01_PW065
Major/Minor Ions								
Aluminum (Al)	mmol/kgw	0.26	0.08	0.44	0.25	0.04	0.39	1.62
Boron (B)	mmol/kgw	17.97	8.25	16.17	20.35	2.02	32.29	2.91
Bromine (Br)	mmol/kgw	17.34	18.47	25.33	20.90	26.87	21.89	23.54
Calcium (Ca)	mmol/kgw	532.10	600.86	1322.71	853.44	1722.95	1060.58	1273.68
Chlorine (Cl)	mmol/kgw	4413.18	4473.88	5741.60	5091.85	5996.85	5410.47	4998.02
Iodine (I)	mmol/kgw	0.07	0.06	0.06	0.06	0.07	0.08	0.08
Iron (Fe)	mmol/kgw	0.01	0.00	0.04	0.02	0.01	0.03	0.01
Lithium (Li)	mmol/kgw	2.68	2.06	3.48	0.74	0.99	0.92	0.28
Magnesium (Mg)	mmol/kgw	227.29	186.95	635.93	451.50	513.19	352.60	223.73
Manganese (Mn)	mmol/kgw	0.01	0.01	0.02	0.02	0.08	0.08	0.15
Potassium (K)	mmol/kgw	272.63	270.69	55.19	129.58	50.60	172.71	150.73
Rubidium (Rb)	mmol/kgw	0.07	0.05	0.02	0.05	0.02	0.08	0.06
Silicon (Si)	mmol/kgw	162.45	61.78	12.55	6.89	26.88	16.40	1.03
Sodium (Na)	mmol/kgw	2740.85	2677.52	2043.98	2687.38	2357.30	2767.80	2205.16
Strontium (Sr)	mmol/kgw	8.49	6.93	24.63	12.66	14.21	19.95	12.04
Sulfur (S)	mmol/kgw	132.21	61.36	267.01	191.45	474.44	221.65	197.21
Environmental Isotopes								
$\delta^{18}O$	‰VSMOW	-6.9	-6.7	-2.3	-7.5	-3.8	-7.2	-5.3
$\delta^{2}H$	‰VSMOW	-40.5	-39.4	-38.5	-38.9	-33.1	-40.6	-37.4
Radiohalides and Strontium Isotopes								
Chlorine-37 ($\delta^{37}Cl$)	‰ SMOC	0.19	0.16	0.07	0.11	0.30	0.20	0.27
Chlorine-36 ($^{36}Cl/Cl$)	--	1.99E-15	2.41E-15	1.76E-15	1.50E-15	1.49E-15	3.16E-15	3.14E-15
Iodine-129 (^{129}I)	atoms/kgw	8.66E-02	2.56E-01	5.42E-02	7.12E-02	5.62E-01	7.35E-02	5.26E-01
Strontium isotope ratio ($^{87}Sr/^{86}Sr$)	--	0.70927	0.70897	0.70929	0.70939	0.70975	0.70947	0.71037
BDL = Below Detection Limit								

Sample ID		SB_BH01_PW066	SB_BH01_AR013
Major/Minor Ions			
Aluminum (Al)	mmol/kgw	92.93	0.02
Boron (B)	mmol/kgw	80.83	0.80
Bromine (Br)	mmol/kgw	9.55	3.11
Calcium (Ca)	mmol/kgw	516.08	251.43
Chlorine (Cl)	mmol/kgw	3323.91	1914.44
Iodine (I)	mmol/kgw	0.00	0.00
Iron (Fe)	mmol/kgw	0.21	0.00
Lithium (Li)	mmol/kgw	1.33	1.06
Magnesium (Mg)	mmol/kgw	47.48	58.80
Manganese (Mn)	mmol/kgw	0.03	0.00
Potassium (K)	mmol/kgw	44.96	19.63
Rubidium (Rb)	mmol/kgw	0.01	0.01
Silicon (Si)	mmol/kgw	114.56	9.53
Sodium (Na)	mmol/kgw	2661.36	1292.24
Strontium (Sr)	mmol/kgw	3.22	2.05
Sulfur (S)	mmol/kgw	12.81	22.30
Environmental Isotopes			
$\delta^{18}O$	‰VSMOW	-7.4	-7.2
$\delta^{2}H$	‰VSMOW	-38.3	-58.2
Radiohalides and Strontium Isotopes			
Chlorine-37 ($\delta^{37}Cl$)	‰ SMOC	0.24	-0.30
Chlorine-36 ($^{36}Cl/Cl$)	--	6.08E-15	8.93E-16
Iodine-129 (^{129}I)	atoms/kgw	7.54E-03	3.93E+00
Strontium isotope ratio ($^{87}Sr/^{86}Sr$)	--	0.71311	0.70837
BDL = Below Detection Limit			

Appendix B.2 Porewater Sample Results - Paper Absorption (PA) Method

Sample ID		SB_BH01_PW003	SB_BH01_PW007	SB_BH01_PW009	SB_BH01_PW011	SB_BH01_PW013	SB_BH01_PW015	SB_BH01_PW017
Major/Minor Ions								
Barium (Ba)	mmol/kgw	0.001	0.006	0.041	0.004	0.003	0.005	0.001
Bromine (Br)	mmol/kgw	0.00	3.09	7.04	27.12	0.47	1.05	0.37
Calcium (Ca)	mmol/kgw	0.47	129.16	94.83	84.16	3.54	7.56	4.36
Chlorine (Cl)	mmol/kgw	0.88	904.40	1945.77	5990.89	363.23	648.71	451.69
Lithium (Li)	mmol/kgw	0.004	0.958	2.222	10.149	0.178	0.375	0.145
Magnesium (Mg)	mmol/kgw	4.13	60.69	54.49	408.31	20.77	25.02	25.58
Potassium (K)	mmol/kgw	BDL	5.18	19.06	41.41	1.64	2.81	BDL
Sodium (Na)	mmol/kgw	0.88	620.00	1844.80	3759.52	305.85	544.85	458.03
Strontium (Sr)	mmol/kgw	0.26	1.12	0.80	6.41	0.46	0.65	0.30
Sulfate (SO_4)	mmol/kgw	7.03	23.36	55.66	34.52	34.49	19.70	46.77
Radiohalides and Strontium Isotopes								
Strontium isotope ratio ($^{87}Sr/^{86}Sr$)	--	0.708306	0.708621	0.708598	0.708539	0.708807	0.708511	0.708865

BDL = Below Detection Limit

Appendix B.2 Porewater Sample Results - Paper Absorption (PA) Method

Sample ID		SB_BH01_PW019	SB_BH01_PW023	SB_BH01_PW025	SB_BH01_PW026	SB_BH01_PW029	SB_BH01_PW030	SB_BH01_PW032
Major/Minor Ions								
Barium (Ba)	mmol/kgw	0.034	0.020	0.032	0.070	0.077	0.049	0.027
Bromine (Br)	mmol/kgw	2.85	7.32	55.54	59.93	74.59	57.17	53.45
Calcium (Ca)	mmol/kgw	125.55	552.40	2162.54	2441.03	2888.46	2444.02	2309.09
Chlorine (Cl)	mmol/kgw	3086.64	5031.83	9674.88	10438.96	12128.20	10021.30	9352.21
Lithium (Li)	mmol/kgw	0.631	2.307	8.089	8.524	9.787	7.777	7.282
Magnesium (Mg)	mmol/kgw	64.78	207.60	405.53	435.92	452.59	423.64	397.46
Potassium (K)	mmol/kgw	12.04	57.40	108.39	107.63	123.25	103.19	87.96
Sodium (Na)	mmol/kgw	3014.04	3861.44	4409.84	4638.87	5521.90	4449.70	3974.75
Strontium (Sr)	mmol/kgw	1.03	6.33	15.58	19.95	25.29	21.57	20.76
Sulfate (SO_4)	mmol/kgw	131.50	17.68	42.92	46.68	46.04	37.28	40.47
Radiohalides and Strontium Isotopes								
Strontium isotope ratio ($^{87}Sr/^{86}Sr$)	--	0.709079	0.709762	0.709870	0.709919	0.709975	0.710008	0.710002

BDL = Below Detection Limit

Appendix B.2 Porewater Sample Results - Paper Absorption (PA) Method

Sample ID		SB_BH01_PW033	SB_BH01_PW036	SB_BH01_PW038	SB_BH01_PW040	SB_BH01_PW041	SB_BH01_PW044	SB_BH01_PW047
Major/Minor Ions								
Barium (Ba)	mmol/kgw	0.069	0.094	0.119	0.183	0.091	0.134	0.209
Bromine (Br)	mmol/kgw	71.91	67.76	78.55	82.27	68.37	77.96	72.18
Calcium (Ca)	mmol/kgw	2905.12	2559.75	2746.37	1702.89	2598.16	2548.76	2691.74
Chlorine (Cl)	mmol/kgw	11596.27	10567.90	11983.10	13230.67	11015.17	11641.85	14674.04
Lithium (Li)	mmol/kgw	9.623	9.302	11.123	18.371	10.852	13.302	15.330
Magnesium (Mg)	mmol/kgw	455.94	369.84	368.93	381.08	607.10	500.05	798.48
Potassium (K)	mmol/kgw	108.66	99.40	113.41	151.11	93.38	105.99	147.06
Sodium (Na)	mmol/kgw	4932.65	4649.31	5568.49	8359.14	4585.76	5480.95	7209.85
Strontium (Sr)	mmol/kgw	29.73	26.87	27.98	15.48	27.96	27.89	31.10
Sulfate (SO_4)	mmol/kgw	51.01	35.22	39.06	25.01	36.85	22.00	514.57
Radiohalides and Strontium Isotopes								
Strontium isotope ratio ($^{87}Sr/^{86}Sr$)	--	0.710024	0.710031	0.710034	0.709948	0.709979	0.709983	0.709802

BDL = Below Detection Limit

Sample ID		SB_BH01_PW049	SB_BH01_PW052	SB_BH01_PW054	SB_BH01_PW056	SB_BH01_PW058	SB_BH01_PW060	SB_BH01_PW063
Major/Minor Ions								
Barium (Ba)	mmol/kgw	0.128	0.125	0.153	0.185	0.134	0.095	0.036
Bromine (Br)	mmol/kgw	49.68	77.45	101.82	57.64	74.89	40.66	50.94
Calcium (Ca)	mmol/kgw	2228.10	1853.89	1001.42	2401.21	2872.66	186.96	2360.38
Chlorine (Cl)	mmol/kgw	8927.63	10803.40	13979.40	10004.70	11539.83	7510.93	8573.14
Lithium (Li)	mmol/kgw	7.710	10.853	19.201	6.072	4.110	2.219	2.072
Magnesium (Mg)	mmol/kgw	456.92	209.69	96.52	705.35	744.60	580.84	398.32
Potassium (K)	mmol/kgw	83.80	101.45	164.29	57.52	63.17	35.66	50.34
Sodium (Na)	mmol/kgw	3793.01	6465.28	11361.84	3935.47	4628.79	2822.61	3158.76
Strontium (Sr)	mmol/kgw	27.46	20.68	9.25	28.85	34.53	18.90	28.42
Sulfate (SO_4)	mmol/kgw	45.17	26.55	18.50	35.79	55.45	32.16	34.42
Radiohalides and Strontium Isotopes								
Strontium isotope ratio ($^{87}Sr/^{86}Sr$)	--	0.709902	0.710049	0.709911	0.709794	0.709895	0.709909	0.710051

BDL = Below Detection Limit

	Sample ID	SB_BH01_NG001	SB_BH01_NG002	SB_BH01_NG004	SB_BH01_NG005	SB_BH01_NG006	SB_BH01_NG007	SB_BH01_NG008
Noble Gas Concentrations								
Helium (He) - total	cc/ccw	8.13E-07	1.30E-05	3.19E-04	9.60E-04	7.87E-04	2.48E-04	2.16E-04
^{4}He	cc/ccw	8.13E-07	1.30E-05	3.19E-04	9.60E-04	7.87E-04	2.48E-04	2.16E-04
^{3}He	cc/ccw	1.17E-12	2.49E-11	1.03E-11	4.29E-11	3.82E-11	1.53E-11	1.14E-11
Neon (Ne) - total	cc/ccw	2.24E-06	4.03E-05	1.05E-06	9.10E-06	1.01E-06	1.84E-06	1.05E-05
^{20}Ne	cc/ccw	2.04E-06	3.64E-05	9.54E-07	8.25E-06	9.14E-07	1.67E-06	9.49E-06
^{22}Ne	cc/ccw	2.03E-07	3.84E-06	9.65E-08	8.50E-07	9.32E-08	1.69E-07	9.69E-07
Argon (Ar) - total	cc/ccw	5.40E-02	2.95E+00	3.29E-02	1.17E+01	7.90E-01	4.81E-02	4.10E-01
^{40}Ar	cc/ccw	5.38E-02	2.94E+00	3.28E-02	1.17E+01	7.88E-01	4.80E-02	4.08E-01
^{36}Ar	cc/ccw	1.77E-04	9.52E-03	9.91E-05	3.61E-02	2.38E-03	1.54E-04	1.49E-03
Krypton (Kr) - total	cc/ccw	6.04E-04	6.00E-03	3.08E-04	6.09E-03	3.72E-04	9.10E-04	5.36E-04
Xenon (Xe) - total	cc/ccw	7.57E-08	2.07E-07	2.09E-08	2.73E-07	9.08E-09	8.08E-08	9.69E-08
Noble Gas Isotopic Ratios								
$^{3}He/^{4}He$ (air-normalized, xRa)	--	1.05E+00	1.38E+00	2.35E-02	3.23E-02	3.52E-02	4.48E-02	3.84E-02
$^{22}Ne/^{20}Ne$	--	9.97E-02	1.06E-01	1.01E-01	1.03E-01	1.02E-01	1.01E-01	1.02E-01
$^{40}Ar/^{36}Ar$	--	3.0E+02	3.1E+02	3.3E+02	3.2E+02	3.3E+02	3.1E+02	2.7E+02

NV = Not reported or no value measured

Sample ID		SB_BH01_NG009	SB_BH01_NG010	SB_BH01_NG012	SB_BH01_NG013	SB_BH01_NG014	SB_BH01_NG015	SB_BH01_NG016
Noble Gas Concentrations								
Helium (He) - total	cc/ccw	3.03E-04	7.59E-04	2.47E-03	4.22E-03	3.09E-03	3.21E-03	1.50E-02
^{4}He	cc/ccw	3.03E-04	7.59E-04	2.47E-03	4.22E-03	3.09E-03	3.21E-03	1.50E-02
^{3}He	cc/ccw	1.19E-11	3.71E-11	9.68E-11	1.64E-10	1.12E-10	1.08E-10	1.57E-08
Neon (Ne) - total	cc/ccw	2.19E-06	1.57E-05	3.50E-06	3.57E-06	3.70E-06	1.39E-06	1.32E-04
^{20}Ne	cc/ccw	1.99E-06	1.42E-05	3.18E-06	3.24E-06	3.36E-06	1.27E-06	1.19E-04
^{22}Ne	cc/ccw	2.02E-07	1.46E-06	3.20E-07	3.37E-07	3.43E-07	1.26E-07	1.28E-05
Argon (Ar) - total	cc/ccw	2.14E+00	6.01E-01	1.04E-01	1.34E-01	1.44E-01	2.14E+00	6.62E+00
^{40}Ar	cc/ccw	2.13E+00	5.99E-01	1.04E-01	1.34E-01	1.44E-01	2.13E+00	6.60E+00
^{36}Ar	cc/ccw	6.98E-03	1.94E-03	3.15E-04	2.38E-04	2.05E-04	5.47E-03	2.10E-02
Krypton (Kr) - total	cc/ccw	1.19E-03	1.75E-03	6.94E-04	1.48E-04	5.54E-04	6.18E-05	3.29E-02
Xenon (Xe) - total	cc/ccw	8.21E-08	2.33E-07	5.94E-08	2.82E-08	6.67E-08	8.17E-09	1.86E-06
Noble Gas Isotopic Ratios								
$^{3}He/^{4}He$ (air-normalized, xRa)	--	2.84E-02	3.54E-02	2.84E-02	2.82E-02	2.62E-02	2.44E-02	7.56E-01
$^{22}Ne/^{20}Ne$	--	1.01E-01	1.03E-01	1.00E-01	1.04E-01	1.02E-01	9.94E-02	1.07E-01
$^{40}Ar/^{36}Ar$	--	3.1E+02	3.1E+02	3.3E+02	5.6E+02	7.0E+02	3.9E+02	3.1E+02

NV = Not reported or no value measured

	Sample ID	SB_BH01_NG017	SB_BH01_NG018	SB_BH01_NG020	SB_BH01_NG021	SB_BH01_NG022	SB_BH01_NG024	SB_BH01_NG025
Noble Gas Concentrations								
Helium (He) - total	cc/ccw	3.88E-03	2.28E-02	4.87E-02	2.28E-02	4.67E-03	4.73E-02	1.63E-02
^{4}He	cc/ccw	3.88E-03	2.28E-02	4.87E-02	2.28E-02	4.67E-03	4.73E-02	1.63E-02
^{3}He	cc/ccw	1.73E-10	8.34E-10	2.23E-09	8.67E-10	2.04E-10	1.65E-09	8.74E-10
Neon (Ne) - total	cc/ccw	6.47E-06	8.61E-06	2.90E-05	2.47E-05	9.12E-06	1.36E-04	5.33E-05
^{20}Ne	cc/ccw	5.91E-06	7.82E-06	2.63E-05	2.24E-05	8.26E-06	1.24E-04	4.84E-05
^{22}Ne	cc/ccw	5.65E-07	7.93E-07	2.69E-06	2.27E-06	8.68E-07	1.24E-05	4.90E-06
Argon (Ar) - total	cc/ccw	5.81E+00	7.99E+00	1.10E+00	9.59E-01	3.64E-01	5.23E+00	1.10E+00
^{40}Ar	cc/ccw	5.81E+00	7.98E+00	1.10E+00	9.58E-01	3.64E-01	5.22E+00	1.10E+00
^{36}Ar	cc/ccw	6.96E-03	9.76E-03	1.12E-03	1.01E-03	3.87E-04	8.92E-03	2.87E-03
Krypton (Kr) - total	cc/ccw	4.37E-04	7.19E-04	7.96E-03	1.75E-03	4.23E-04	3.53E-03	5.27E-03
Xenon (Xe) - total	cc/ccw	5.85E-08	9.18E-08	6.84E-07	2.68E-07	9.64E-08	1.23E-06	3.48E-07
Noble Gas Isotopic Ratios								
$^{3}He/^{4}He$ (air-normalized, xRa)	--	3.23E-02	2.66E-02	3.31E-02	2.76E-02	3.17E-02	2.53E-02	3.89E-02
$^{22}Ne/^{20}Ne$	--	9.56E-02	1.01E-01	1.02E-01	1.01E-01	1.05E-01	1.00E-01	1.01E-01
$^{40}Ar/^{36}Ar$	--	8.3E+02	8.2E+02	9.8E+02	9.5E+02	9.4E+02	5.9E+02	3.8E+02

NV = Not reported or no value measured

Appendix B.3 Noble Gas Sample Results

	Sample ID	SB_BH01_NG026	SB_BH01_NG027	SB_BH01_NG028	SB_BH01_NG029	SB_BH01_NG030	SB_BH01_NG032	SB_BH01_NG033
Noble Gas Concentrations								
Helium (He) - total	cc/ccw	3.28E-02	1.97E-02	7.71E-02	2.48E-02	7.34E-03	7.46E-03	6.99E-02
^{4}He	cc/ccw	3.28E-02	1.97E-02	7.71E-02	2.48E-02	7.34E-03	7.46E-03	6.99E-02
^{3}He	cc/ccw	3.01E-09	1.57E-09	6.41E-09	1.75E-09	6.50E-10	5.65E-10	4.94E-09
Neon (Ne) - total	cc/ccw	1.75E-03	1.91E-05	2.28E-04	6.28E-05	7.69E-06	1.37E-05	1.83E-05
^{20}Ne	cc/ccw	1.58E-03	1.73E-05	2.07E-04	5.71E-05	6.96E-06	1.25E-05	1.65E-05
^{22}Ne	cc/ccw	1.74E-04	1.75E-06	2.12E-05	5.74E-06	7.30E-07	1.22E-06	1.78E-06
Argon (Ar) - total	cc/ccw	1.08E+02	5.79E-01	2.21E+00	2.34E+00	3.07E-01	5.54E-01	6.73E-01
^{40}Ar	cc/ccw	1.08E+02	5.78E-01	2.21E+00	2.33E+00	3.07E-01	5.53E-01	6.73E-01
^{36}Ar	cc/ccw	3.40E-01	5.69E-04	5.63E-03	1.70E-03	9.26E-05	3.79E-04	2.13E-04
Krypton (Kr) - total	cc/ccw	1.72E-01	1.50E-03	2.85E-02	2.29E-03	8.73E-04	1.09E-04	9.38E-04
Xenon (Xe) - total	cc/ccw	8.68E-06	1.81E-07	1.12E-06	5.41E-07	1.49E-07	9.76E-08	1.63E-07
Noble Gas Isotopic Ratios								
^{3}He/^{4}He (air-normalized, xRa)	--	6.65E-02	5.78E-02	6.03E-02	5.10E-02	6.41E-02	5.49E-02	5.13E-02
^{22}Ne/^{20}Ne	--	1.10E-01	1.01E-01	1.02E-01	1.01E-01	1.05E-01	9.82E-02	1.07E-01
^{40}Ar/^{36}Ar	--	3.2E+02	1.0E+03	3.9E+02	1.4E+03	3.3E+03	1.5E+03	3.2E+03

NV = Not reported or no value measured

	Sample ID	SB_BH01_NG034
Noble Gas Concentrations		
Helium (He) - total	cc/ccw	1.27E-02
^{4}He	cc/ccw	1.27E-02
^{3}He	cc/ccw	1.02E-09
Neon (Ne) - total	cc/ccw	1.58E-04
^{20}Ne	cc/ccw	1.43E-04
^{22}Ne	cc/ccw	1.49E-05
Argon (Ar) - total	cc/ccw	6.30E+00
^{40}Ar	cc/ccw	6.28E+00
^{36}Ar	cc/ccw	2.13E-02
Krypton (Kr) - total	cc/ccw	8.16E-04
Xenon (Xe) - total	cc/ccw	1.12E-06
Noble Gas Isotopic Ratios		
^{3}He/^{4}He (air-normalized, xRa)	--	5.81E-02
^{22}Ne/^{20}Ne	--	1.04E-01
^{40}Ar/^{36}Ar	--	2.9E+02

NV = Not reported or no value measured

	Sample ID	SB_BH01_DG001	SB_BH01_DG002	SB_BH01_DG004	SB_BH01_DG005	SB_BH01_DG006	SB_BH01_DG007	SB_BH01_DG008	SB_BH01_DG009
Carbon Dioxide and Methane Concentrations									
CO_2	mmol/kgw	1.04E+00	1.13E+00	1.23E-02	6.36E-01	8.89E-01	2.47E-01	4.01E+00	2.70E-02
CH_4	mmol/kgw	BDL	BDL	4.91E-03	7.24E-02	8.39E-03	2.69E-03	1.82E-02	BDL
Carbon Dioxide and Methane Isotopic Ratios									
δ^{13} CO_2	VPDB (‰)	-7.3	-11.0	-16.0	-7.0	-4.9	-8.0	-5.4	-3.4
δ^{13}C CH_4	VPDB (‰)	BDL	BDL	-40.6	-47.1	-51.3	BDL	BDL	BDL
δ^{2}H CH_4	VSMOW (‰)	BDL	BDL	BDL	BDL	-221	BDL	BDL	BDL

BDL = below detection limit

Sample ID		SB_BH01_DG010	SB_BH01_DG012	SB_BH01_DG013	SB_BH01_DG014	SB_BH01_DG015	SB_BH01_DG016	SB_BH01_DG017	SB_BH01_DG018
Carbon Dioxide and Methane Concentrations									
CO_2	mmol/kgw	7.40E+00	3.41E-02	4.09E-01	5.52E-01	9.04E-01	6.79E-01	1.36E+00	1.43E+00
CH_4	mmol/kgw	5.49E-02	BDL	2.99E-01	5.98E-01	1.29E+00	1.15E+00	5.55E+00	1.31E+01
Carbon Dioxide and Methane Isotopic Ratios									
δ^{13} CO_2	VPDB (‰)	-3.2	-3.1	-6.0	-3.9	-3.9	-4.8	5.4	5.2
$\delta^{13}C$ CH_4	VPDB (‰)	BDL	BDL	-46.0	-45.8	-46.7	-46.9	-46.7	-46.2
$\delta^{2}H$ CH_4	VSMOW (‰)	BDL	BDL	-232	-229	-251	-246	-261	-259

BDL = below detection limit

Sample ID		SB_BH01_DG019	SB_BH01_DG020	SB_BH01_DG021	SB_BH01_DG022	SB_BH01_DG024	SB_BH01_DG025	SB_BH01_DG026	SB_BH01_DG027
Carbon Dioxide and Methane Concentrations									
CO_2	mmol/kgw	7.38E-01	7.05E-01	8.02E-01	5.20E-01	2.05E+01	1.14E+00	1.30E+00	1.46E+00
CH_4	mmol/kgw	2.18E+01	3.74E+01	8.93E+00	5.58E+00	1.82E+02	1.09E+01	1.44E+01	1.06E+01
Carbon Dioxide and Methane Isotopic Ratios									
δ^{13} CO_2	VPDB (‰)	5.7	-4.8	-4.3	-5.0	3.5	-3.6	-4.6	-2.9
$\delta^{13}C$ CH_4	VPDB (‰)	-46.2	-46.2	-45.5	-44.4	-43.2	-42.0	-40.0	-40.6
$\delta^{2}H$ CH_4	VSMOW (‰)	-257	-258	-250	-249	-227	-221	-214	-191

BDL = below detection limit

Appendix B.3 Dissolved Gas Sample Results

Sample ID		SB_BH01_DG028	SB_BH01_DG029	SB_BH01_DG030	SB_BH01_DG032	SB_BH01_DG033
Carbon Dioxide and Methane Concentrations						
CO_2	mmol/kgw	5.90E-01	4.53E-01	8.37E-01	6.75E-02	1.26E+00
CH_4	mmol/kgw	BDL	BDL	2.38E+00	6.83E-01	BDL
Carbon Dioxide and Methane Isotopic Ratios						
δ^{13} CO_2	VPDB (‰)	-3.0	-3.4	-2.0	-5.4	-10.8
$\delta^{13}C$ CH_4	VPDB (‰)	BDL	BDL	-38.1	-37.8	BDL
$\delta^{2}H$ CH_4	VSMOW (‰)	BDL	BDL	-183	-176	BDL

BDL = below detection limit

Mineralogical and Petrological Results for Porewater Samples at SB_BH01

C.1. – X-Ray Diffraction Results (XRD)
C.2 – Scanned Thin Sections and Corresponding SEM Images

Appendix C.1. X-Ray Diffraction (XRD) Results for Select Core Porewater Samples

Sample ID	Phase Proportion (%) by Relative Intensity Ratio																
	Calcite	Dolomite	Ankerite	Quartz	Muscovite and/or illite and/or glauconite and/or celadonite	Other micas and/or clays	Clinochlore	Gypsum	Anhydrite	Celestite	Feldspars	Pyrite	Halite	Hematite	Goethite	Anatatse	Sum
SB_BH01_PW003	--	98.10	--	0.30	--	--	--	--	--	1.60	--	--	--	--	--	--	100.00
SB_BH01_PW007	--	27.00	--	17.70	35.90	--	2.60	--	4.80	--	11.90	--	--	--	--	--	99.90
SB_BH01_PW009	--	58.20	--	14.30	15.60	--	2.00	--	--	--	9.20	0.80	--	--	--	--	100.10
SB_BH01_PW011	--	31.20	--	34.00	17.10	--	3.20	--	--	--	14.50	--	--	--	--	--	100.00
SB_BH01_PW013	--	80.90	--	--	--	--	--	--	--	6.20	12.90	--	--	--	--	--	100.00
SB_BH01_PW015	83.90	15.10	--	0.40	--	--	0.60	--	--	--	--	--	--	--	--	--	100.00
SB_BH01_PW017	--	95.10	--	0.90	--	--	--	--	--	--	--	--	1.60	2.50	--	--	100.10
SB_BH01_PW019	17.30	80.90	--	1.60	--	--	--	--	--	--	--	--	--	0.30	--	--	100.10
SB_BH01_PW023	--	--	--	33.60	61.60	--	4.10	--	--	--	--	0.70	--	--	--	--	100.00
SB_BH01_PW025	22.60	--	--	22.50	40.10	8.50	5.60	--	--	--	--	--	--	0.70	--	--	100.00
SB_BH01_PW026	24.70	3.90	--	18.50	47.20	--	5.70	--	--	--	--	--	--	--	--	--	100.00
SB_BH01_PW029	2.80	--	--	24.30	58.70	--	12.10	2.10	--	--	--	--	--	--	--	--	100.00
SB_BH01_PW030	3.70	--	--	49.90	27.90	--	6.70	--	--	--	11.60	--	--	--	--	--	99.80
SB_BH01_PW032	--	--	--	29.90	5.00	4.40	8.00	--	--	--	52.20	--	0.50	--	--	--	100.00
SB_BH01_PW033	--	--	2.40	37.10	45.60	--	12.40	--	--	--	--	2.50	--	--	--	--	100.00
SB_BH01_PW036	Not analysed																
SB_BH01_PW038	7	--	--	60.4	15.4	--	13.8	--	--	--	--	3.5	--	--	--	--	100.1
SB_BH01_PW040	70.9	--	10.9	4.9	5.3	--	1.3	--	--	--	6.6	--	--	--	--	--	99.9
SB_BH01_PW041	51.6	--	27	5.4	5.2	1.6	--	--	--	--	8.9	--	0.4	--	--	--	100.1
SB_BH01_PW044	46.7	9.6	--	10.7	20.7	--	--	--	--	--	11.2	1.1	--	--	--	--	100
SB_BH01_PW047	70.2	26.8	--	0.7	--	--	--	--	--	--	1.8	0.6	--	--	--	--	100.1
SB_BH01_PW049	28.6	--	65.7	1.4	4.4	--	--	--	--	--	--	--	--	--	--	--	100.1
SB_BH01_PW052	71	4.4	--	5.5	9	--	--	--	--	--	8.9	--	--	--	1.2	--	100
SB_BH01_PW054	69.2	--	--	6.6	13	--	0.8	--	--	--	8.3	2	--	--	--	--	99.9
SB_BH01_PW056	69.8	9.2	6.7	13.1	--	--	--	--	--	--	--	--	--	--	1.3	--	100.1
SB_BH01_PW058	Not analysed																
SB_BH01_PW060	Not analysed																
SB_BH01_PW063	1	--	--	33.5	40.7	--	11.5	--	--	--	13.3	--	--	--	--	--	100
SB_BH01_PW067	Not analysed																

-- = not detected or not reported

SB_BH01_PW003 Bass Island
114.08 – 114.27 m

2 × 4 cm

SB_BH01_PW009 Salina E
203.95 - 204.23 m

SB_BH01_PW011 Salina B
229.27 - 229.58 m

SB_BH01_PW013 Salina A2 Carbonate
263.86 - 264.14 m

SB_BH01_PW015 Guelph
307.02 - 307.17 m

SB_BH01_PW017 Guelph
324.24 - 324.49 m

SB_BH01_PW019 Goat Island
344.89 - 345.09 m

SB_BH01_PW023 Cabot Head
401.48 - 401.82 m

SB_BH01_PW033 Blue Mountain
611.86 - 612.08 m

SB_BH01_PW041 Cobourg Fm Lower Mb
665.53 - 665.75 m

SB_BH01_PW049 Sherman Fall
716.6 - 716.81 m

SB_BH01_PW052 Kirkfield
747.75 - 748.02 m

SB_BH01_PW058 Gull River
818.26 - 818.58 m

SB_BH01_PW025 Queenston shale 436.33 – 436.59 m

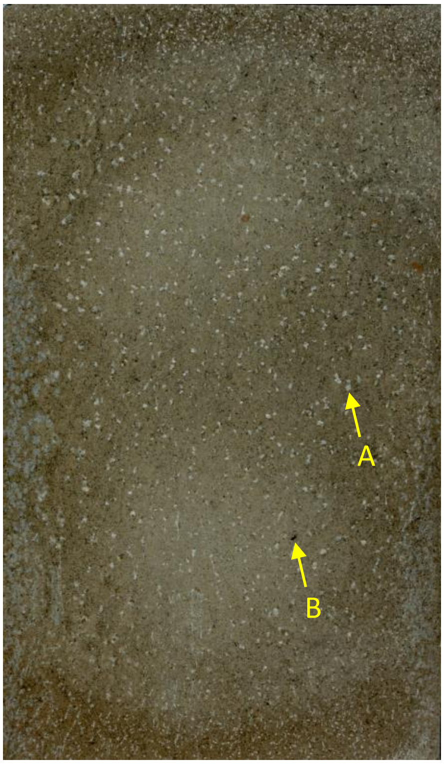

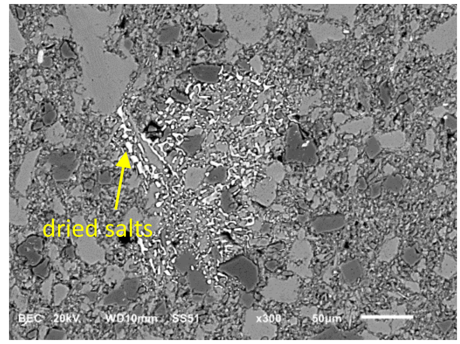

Location A: Light grey spots represent salts, mostly NaCl, precipitated from dried pore water.

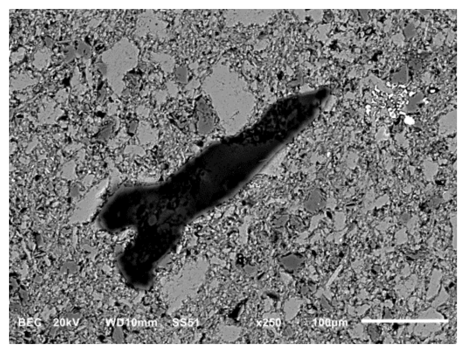

Location B: Black particles in the silty detrital-mineral matrix are organic fragments. Note the precipitated salts in the upper right.

SB_BH01_PW026 Queenston shale 476.28 – 476.59 m

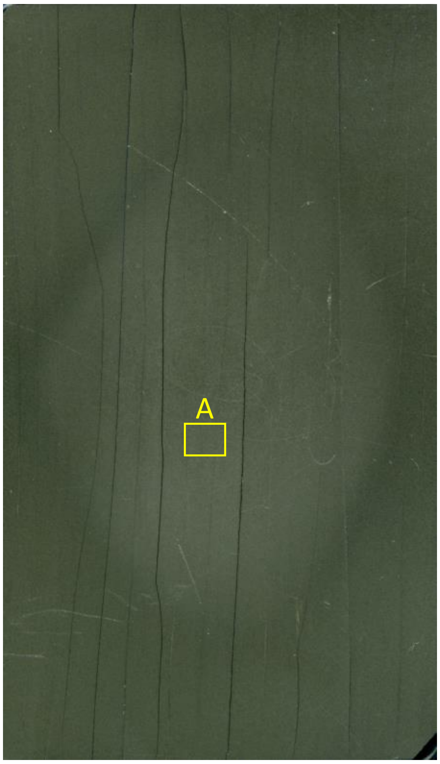

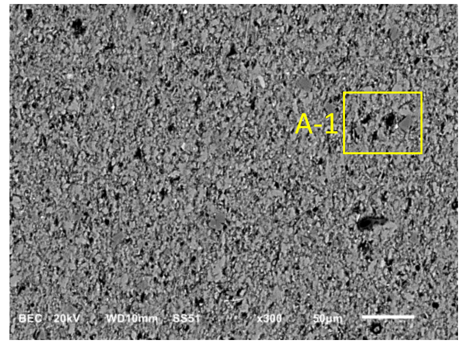

Location A: Uniform, very fine grained detrital matrix with small organic fragments.

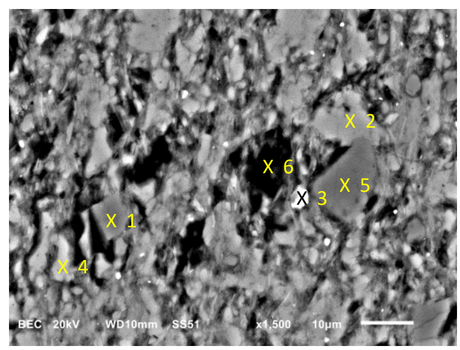

Inset A-1: Fine organic fragments (black) with clay minerals lining the pore walls. Numbers indicate locations of EDS analyses used to identify minerals 1) dolomite, 2) calcite, 3) sphene, 4) calcite, 5) dolomite, 6) organic fragment.

SB_BH01_PW029 Georgian Bay shale 524.71 – 524.92 m

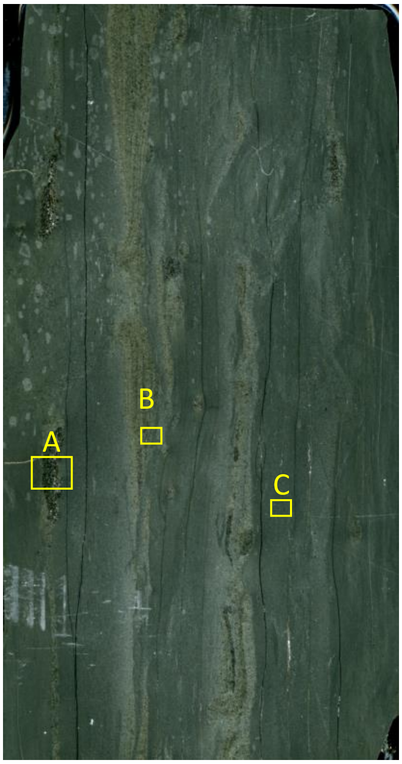

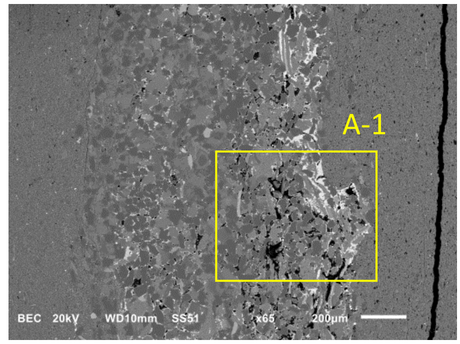

Location A: Silty lens containing organic fragments with diagenetic pyrite.

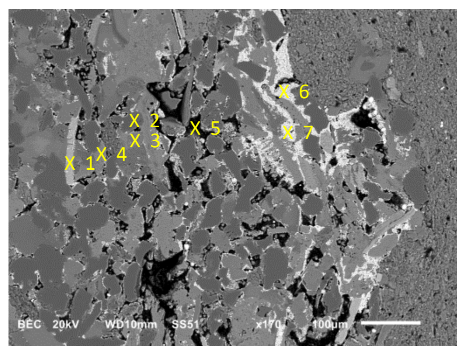

Inset A-1: Higher magnification images of the silty lens with organic fragments (black) and diagenetic pyrite. Numbers indicate locations of EDS analyses used to identify minerals 1) apatite (biogenic?), 2) quartz, 3) mixed Ca-Al-Mg-K silicates, 4) calcite, 5) organic fragment, 6) pyrite, 7) pyrite.

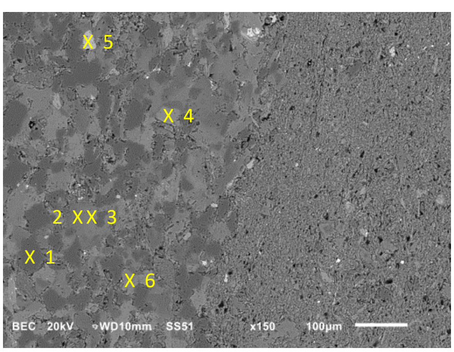

Location B: Carbonate cemented silty lens. Numbers indicate locations of EDS analyses used to identify minerals 1) quartz, 2) dolomite, 3) dolomite (ferroan), 4) calcite, 5) apatite, 6) calcite.

SB_BH01_PW029 Georgian Bay shale 524.71 – 524.92 m continued…

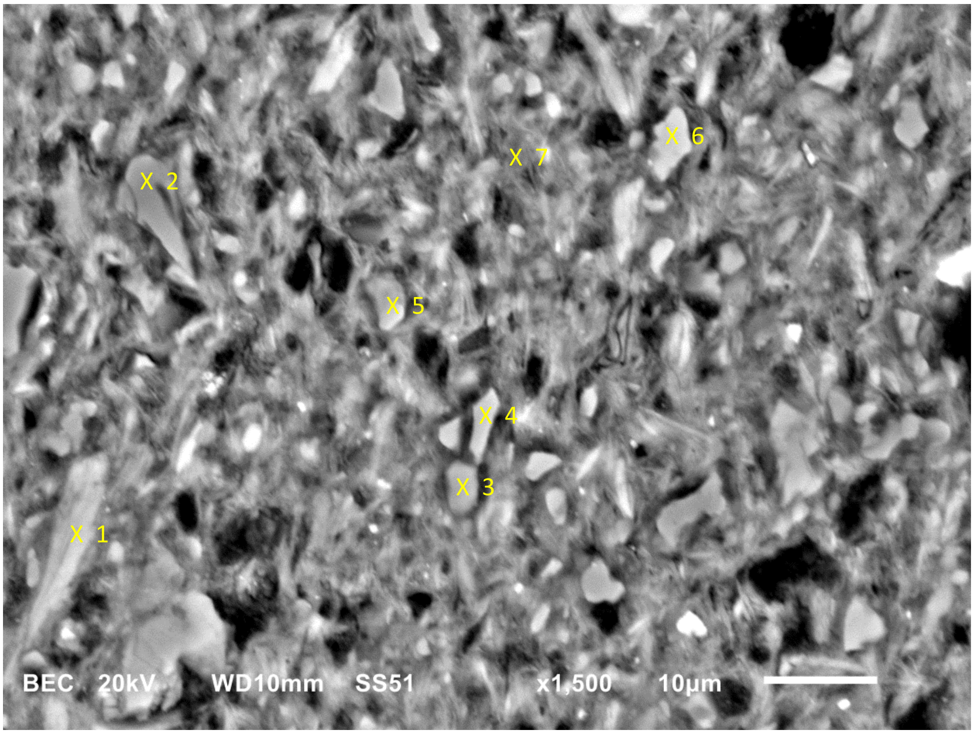

Location C: Very fine-grained shale with detrital minerals, mostly quartz, and clay minerals lining the pores. Numbers indicate locations of EDS analyses used to identify minerals 1) biotite, 2) quartz, 3) quartz, 4) quartz, 5) quartz, 6) K feldspar, 7) clay minerals.

SB_BH01_PW030 Georgian Bay shale 526.8 – 527.06 m

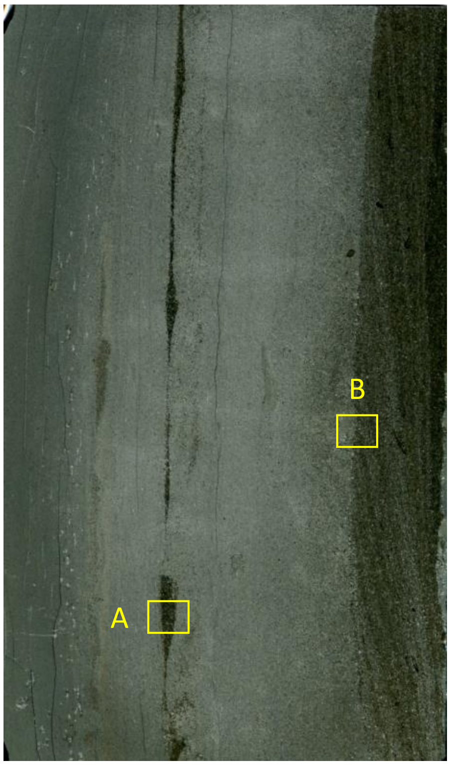

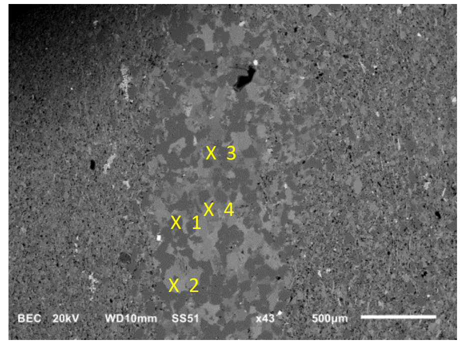

Location A: Silty lens. Numbers indicate locations of EDS analyses used to identify minerals 1) quartz, 2) calcite, 3) dolomite, 4) dolomite.

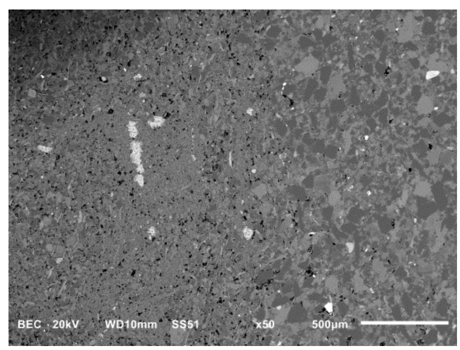

Location B: Boundary between fine-grained shale (left) and silty layer (right). Light grey linearly aligned grains in the centre-left are precipitates from dried porewater.

SB_BH01_PW032 Georgian Bay shale 564.17 – 564.43 m

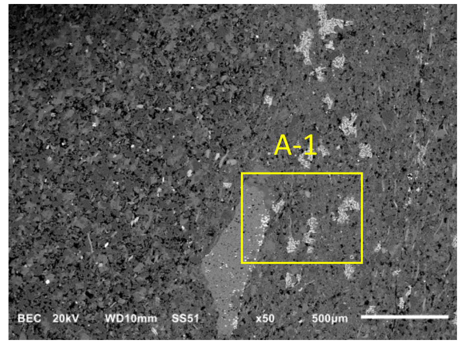

Location A: Boundary between relatively coarse- (left) and fine-grained (right) layers.

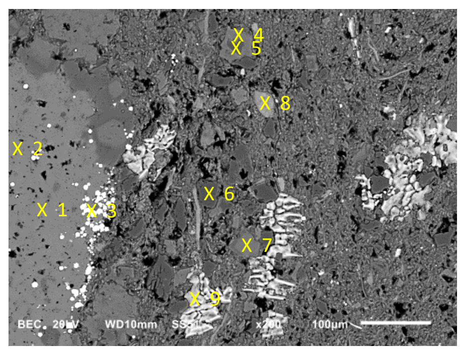

Inset A-1: Higher magnification image from inset shown in A. A calcite fragment is along the left margin, black interstitial material is organic and the large light-grey regions are NaCL precipitates from dried porewater. Numbers indicate locations of EDS analyses used to identify minerals 1) calcite, 2) calcite, 3) pyrite, 4) dolomite (ferroan), 5) dolomite, 6) quartz, 7) dolomite (ferroan), 8) Fe-Mg-Al-silicate, 9) NaCl precipitate from dried porewater.

SB_BH01_PW036 Blue Mountain shale 631.61 – 631.85 m

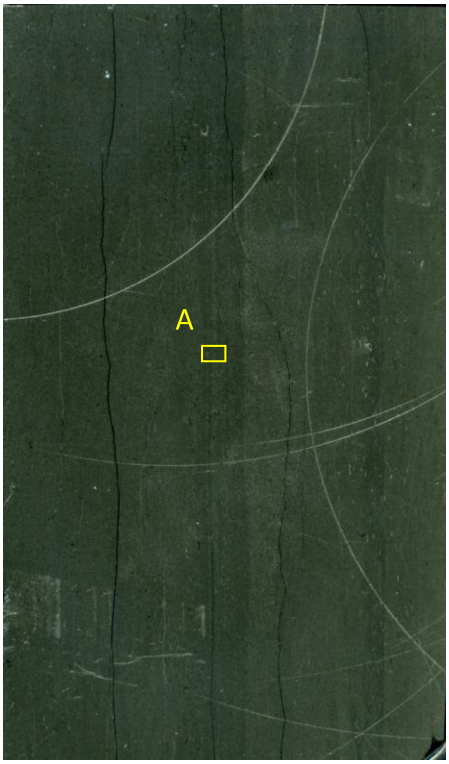

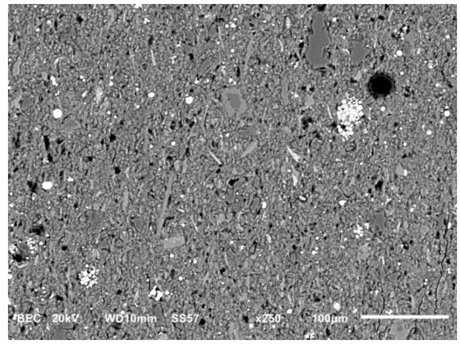

Location A: Fine-grained disseminated euhedral and framboidal pyrite in shale matrix. Typical of the entire section area.

SB_BH01_PW038 Cobourg Fm, Collingwood Mb 637.33 – 637.54 m

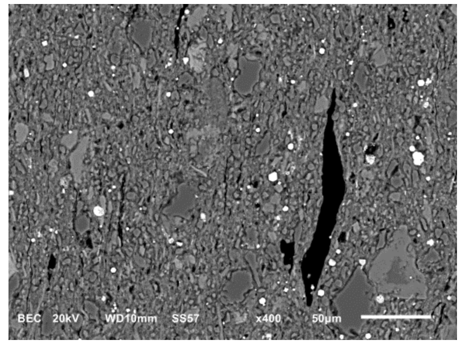

Location A: Fine disseminated pyrite and organic fragments (black) in fine to medium grained shale matrix. Typical of the entire sample area.

SB_BH01_PW040 Cobourg Fm, Collingwood Mb 650.02 – 650.25 m

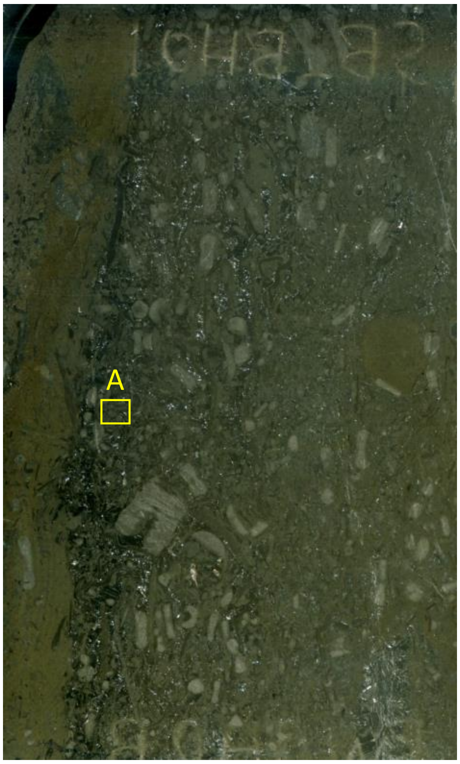

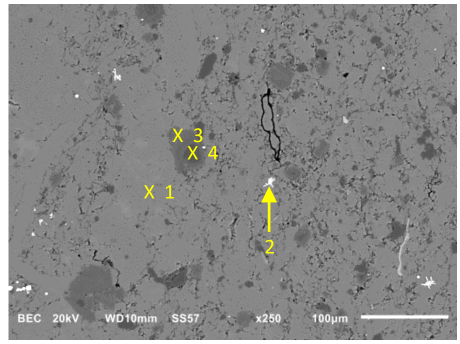

Location A: dominantly calcite with disseminated dolomite and pyrite, and organics (black) infilling pore spaces. Numbers indicate locations of EDS analyses used to identify minerals 1) calcite, 2) pyrite, 3) dolomite (ferroan), 4) dolomite.

SB_BH01_PW044 Cobourg Fm, Lower Mb 683.87 – 684.14 m

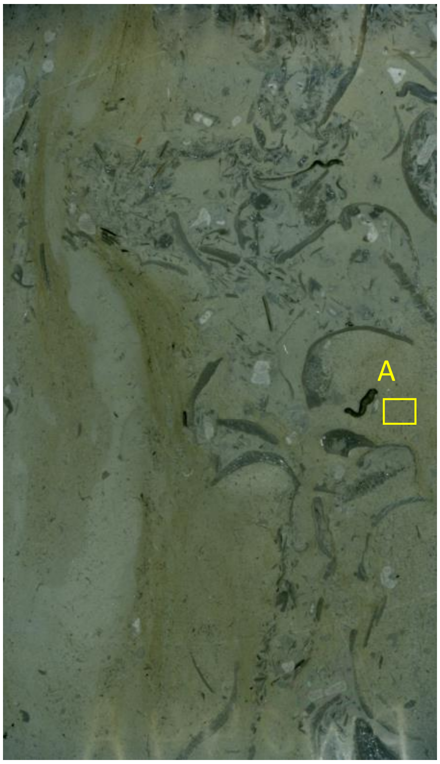

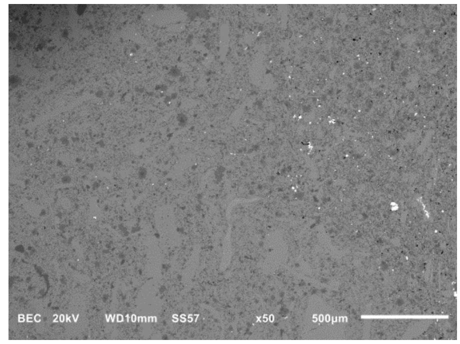

Location A: Micritic matrix to bioclasts. Dominantly calcite with disseminated dolomite (dark grey), pyrite (white), and organics (black).

SB_BH01_PW047 Sherman Fall 693.93 – 694.12 m

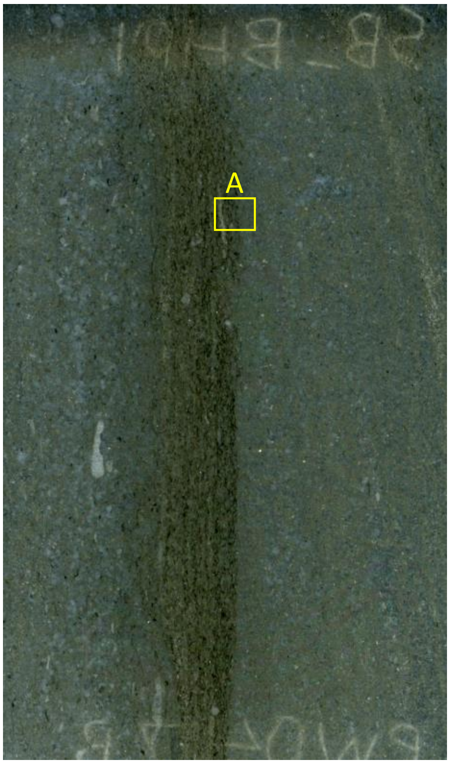

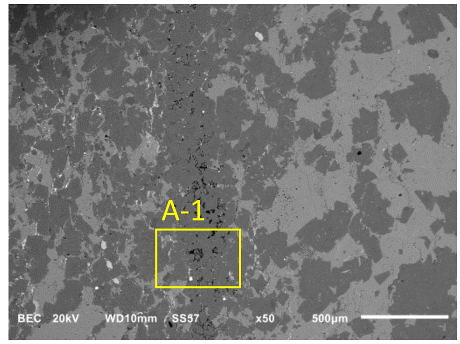

Location A: The boundary observed in the scanned image at left marks the change from relatively coarse calcite-rich matrix at the right to finer dolomite-rich matrix at left. Calcite is light grey, dolomite is dark grey. The dolomite-rich zone has higher porosity (inset) and contains greater abundance of pyrite (disseminated white grains).

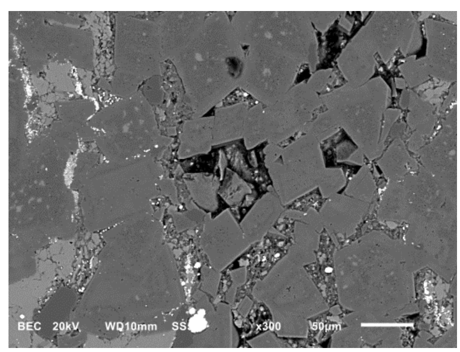

Inset A-1: Porosity likely created by volume change during dolomitization. Pores contain clay minerals. Bright white grains are pyrite, light grey is calcite and dark grey is dolomite.

SB_BH01_PW054 Kirkfield 763.96 – 764.19 m

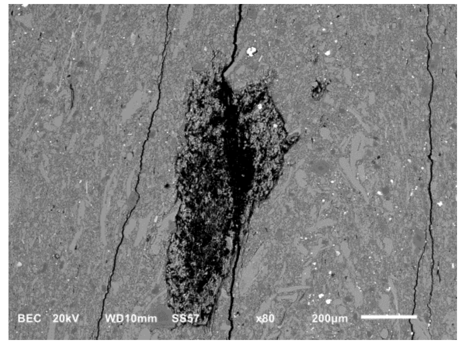

Location A: Organic material (black) infilling porous zone and cross-cutting fracture in micritic and bioclastic matrix.

SB_BH01_PW056 Coboconk 785.86 – 786.12 m

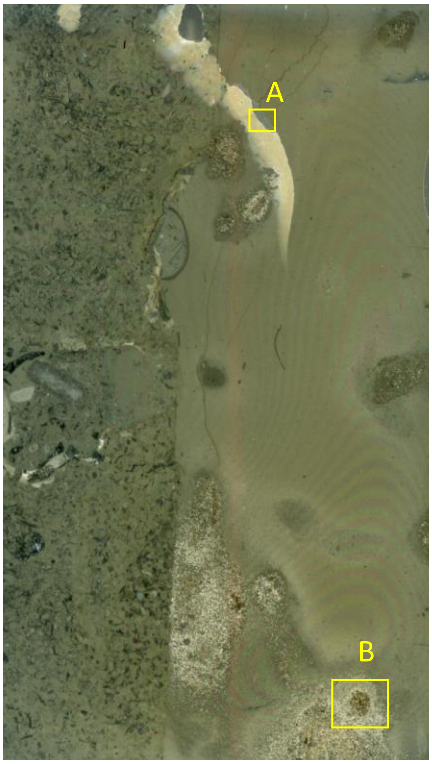

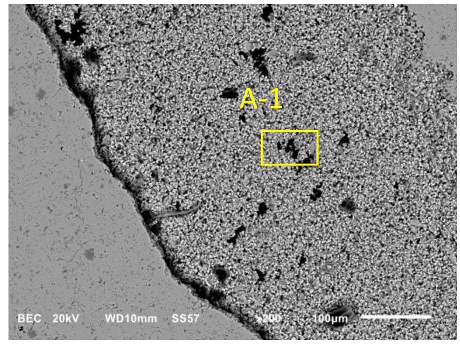

Location A: Porous microcrystalline calcite with organic material (black) infilling largest pores.

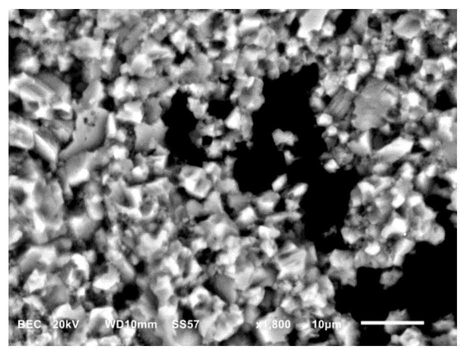

Inset A-1: Porous microcrystalline calcite with organic material (black).

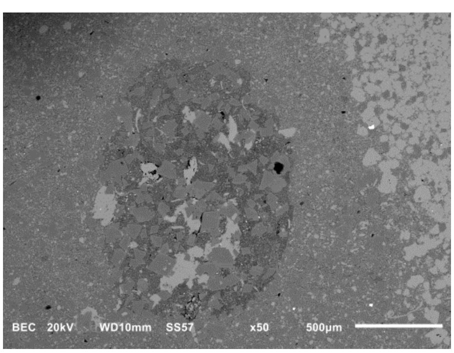

Location B: Siliceous, calcite-rich halo (medium grey) surrounding circular region with relatively large calcite and dolomite grains and organic material in largest pores.

SB_BH01_PW060 Gull River 843.78 – 844.03 m

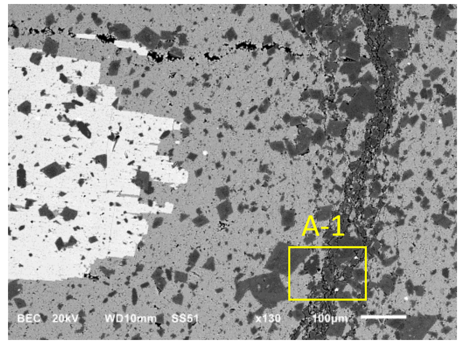

Location A: Calcite matrix (medium grey) has been overprinted by large grains of gypsum/anhydrite (light grey) and dolomite (dark grey). There is gypsum/anhydrite in the fracture near the top and minor pyrite (white) disseminated in the gypsum/anhydrite, in the calcite matrix and in the dolomite. Dolomitization is focused along the near vertical fracture at the right side.

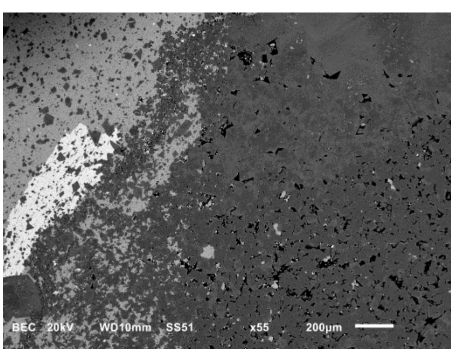

Location B: Calcite matrix and gypsum/anhydrite grain (upper left) are overprinted by dolomite to the point where the material on the right side of the image (oval-shaped features in the scanned colour image) is almost 100% dolomite with organic-filled pores.

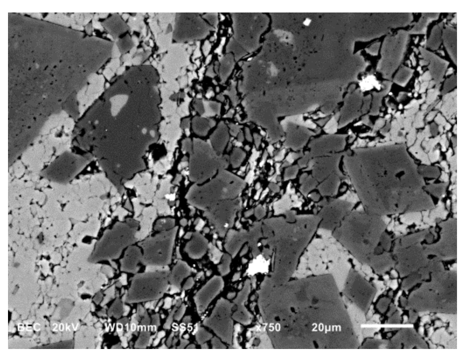

Inset A-1: Higher magnification image of the fracture. The micritic calcite matrix is light grey, pryrite grains are white and the dark grey crystals are dolomite. The fracture contains organics (black), and EDS analyses indicate that it is lined with clay minerals.

SB_BH01_PW063 Shadow Lake 855.29 – 855.5 m

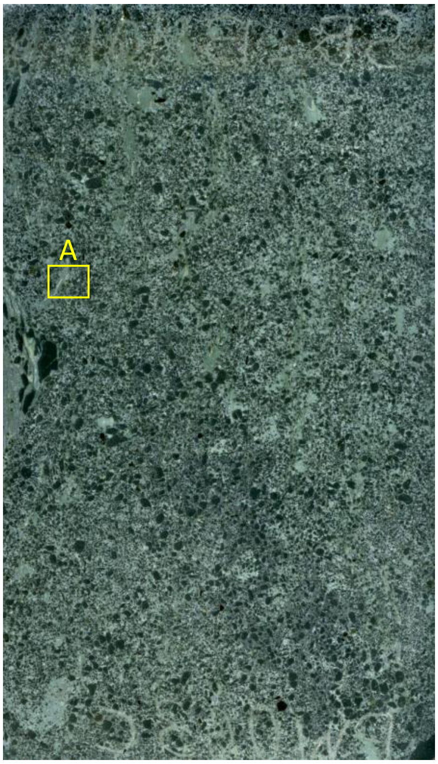

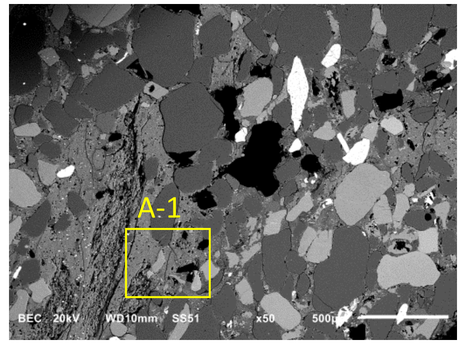

Location A: Rounded detrital grains of quartz (dark grey) K-feldspar (medium grey) and apatite (white). Black organic material fills pores.

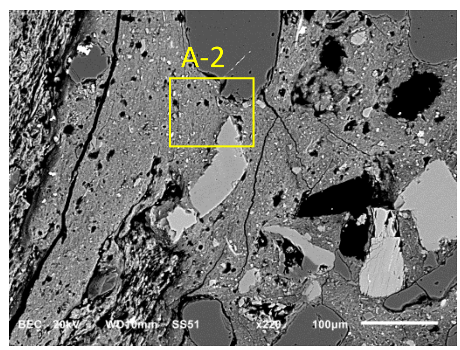

Inset A-1: Higher magnification image showing matrix with a mix detrital grains and cement with clay-composition (Mg-Fe-Si-Al-Ca-K). Clay minerals are evident in the higher magnification image (inset A-2) of the matrix at lower left.

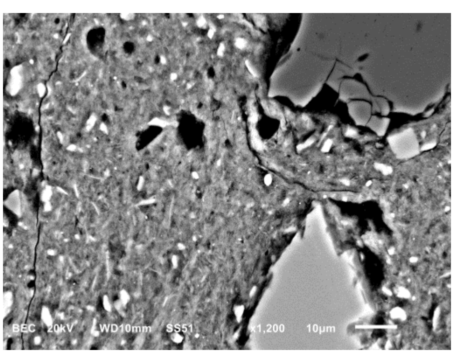

Inset A-2